THE EFFECT OF PHOTOCHEMICAL MODELS ON CALCULATED EQUILIBRIA AND COOLING RATES IN THE STRATOSPHERE

Donna Blake

The Florida State University
Tallahassee, Florida

and

Richard S. Lindzen[1]

Harvard University
Cambridge, Massachusetts

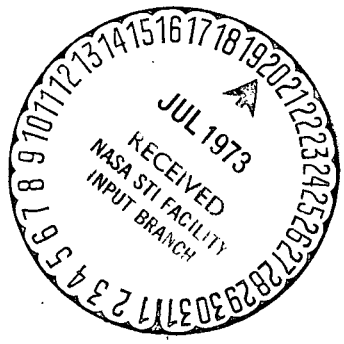

[1] Alfred P. Sloan Foundation Fellow

ABSTRACT

Simplified models are developed for radiative heating and cooling and for ozone photochemistry in the region 22-60 km. The latter permit the inclusion of nitrogen and hydrogen reactions in addition to simple oxygen reactions. The simplicity of the scheme facilitates the use of a wide variety of cooling and reaction rates. We also consider determination of temperature and composition as a joint process. It is shown that joint radiative-photochemical equilibrium is appropriate to the mean state of the atmosphere between 35 and 60 km. Equilibrium calculations are then used to show that hydrogen reactions are important for ozone and temperature distributions primarily above 40 km while nitrogen reactions are important primarily below 50 km. Comparisons with observed distributions of temperature and ozone suggest the need for water vapor mixing ratios of from $0.5\text{-}2.5 \times 10^{-6}$ and mixing ratios of $(NO_2 + NO)$ of from 2×10^{-8}-1.6×10^{-7} at the stratopause. At 35 km, a mixing ratio of $(NO_2 + NO)$ of about 3×10^{-8} is indicated. The precise values depend on our choice of reaction and radiative cooling rate coefficients, and the simple formulation permits the reader to check the effect of new rates as they become available.

The relaxation of perturbations from joint radiative-photochemical equilibrium is also investigated. In all cases the coupling between temperature dependent ozone photochemistry and radiation lead to a reduction of the thermal relaxation time from its purely radiative value. The latter, which amounts to about 10 days, is reduced to 2-4 days at heights of 31-35 km. This greatly enhances the dissipation of waves travelling through the stratosphere.

1. INTRODUCTION

The equilibrium temperature in the stratosphere is determined by the approximate balance between heating due to absorption of solar ultraviolet energy by ozone and cooling due to infrared emission by the 15μ band of carbon dioxide. (A certain amount of cooling is also due to O_3 9.6μ emission, but this cooling is considerably less than that due to the 15μ band of CO_2 [Murgatroyd and Goody 1958]). The rate of energy absorption and therefore the temperature depend on the ozone density.

Production of ozone is by the reaction

$$O + O_2 + M \rightarrow O_3 + M \qquad (A)$$

which is strongly temperature dependent. This coupling between temperature and ozone density indicates that the relaxation time of a temperature perturbation should not be that due to carbon dioxide cooling alone but should be that due to carbon dioxide cooling modified by the effects of photochemistry.

Lindzen and Goody (1965) have calculated the thermal relaxation time for carbon dioxide cooling coupled with photochemical effects for a pure oxygen atmosphere. Since these calculations were made, the rates for pure oxygen reactions have been questioned and alternative rates have been proposed. In addition it now seems that reactions involving nitrogen and hydrogen compounds may be significant in determining the ozone distribution in the stratosphere.

(Hunt 1966, Leovy 1969a, Crutzen 1971) and such reactions should therefore be included in the photochemical model. Most of the rates for reactions involving hydrogen compounds are not temperature dependent so there is a question as to the influence of these reactions on the coupling between ozone density and temperature. It has been suggested (Leovy 1969a) that if the hydrogen reactions are dominant in determining the ozone density then the appropriate thermal relaxation time is just that due to cooling from the 15μ carbon dioxide band. As we shall show, this is untrue since relation (1) remains important in all schemes.

Cooling due to infrared emission by carbon dioxide and modified by photochemistry acts as damping on motions in the stratosphere. The time scale for this damping, which may be represented as Newtonian cooling, is simply the thermal relaxation time scale. As Dickinson (1969) shows, internal Rossby waves, excited in the troposphere, could carry large amounts of energy up to the lower atmosphere unless this time is much less than ten days, ten days being the approximate time scale for unmodified CO_2 15μ cooling. Thus, the effects of photochemistry on this time scale could be crucial.

In this paper we shall investigate the effect of photochemistry on the cooling rate for the height range 22-61 km. A simplified photochemical model that is suitable for this height range and that includes reactions involving nitrogen and hydrogen compounds is developed in section 2. The temperature equation for this photochemical model is obtained in section 3. Vertical distributions of constituents and temperature for radiative-photochemical equilibrium are discussed in section 4. Linearized equations for the photochemistry

and temperature are found in section 5 as are the relevant time scales for photochemical and thermal relaxation. Conclusions are presented in section 6.

Many reaction rates are uncertain by as much as an order of magnitude so a wide range of values is used. Because mixing ratios for water vapor and nitrogen oxides are uncertain several distributions are used. For the range of rates and ratios used, it is found that the effect of including photochemistry is to reduce the thermal relaxation time scale above 30 km from the value appropriate when only infrared emission by carbon dioxide is considered. Furthermore, the minimum value for the thermal relaxation time scale always occurs at heights between 31 and 35 km and with values between two and four days.

It is also found that equilibrium distributions of temperature and ozone density vary with the different rates and ratios assumed. At the stratopause relaxation time scales are short enough ($\sim$90 minutes for ozone and a few days for temperature) that the equilibrium temperature should be close to the observed temperature of approximately 270°K (Supplemental Atmosphere [Tropical], Theon and Smith 1971). We attempt to match the observed temperature rather than the observed ozone densities since the former is better determined than the latter between 35 and 61 km.

The neglect of nitrogen and hydrogen reactions leads to the prediction of excessive temperatures between 35 and 61 km. The prediction of observed temperatures between 50 and 61 km calls for water vapor mixing ratios of from 0.5-3 x 10^{-6} depending on the reaction rates used. A mixing ratio for total nitrogen oxides ($NO + NO_2$) of 2-3 x 10^{-8} produces correct temperatures from 35-50 km. All such estimates depend on our choice of reaction and cooling rate coefficients, but the dependence has been specified in a simple manner.

2. PHOTOCHEMICAL MODEL

As many as 80 different reactions have been considered for an atmosphere consisting of nitrogen, hydrogen, oxygen, and their compounds (Hunt 1966, Shimazaki and Laird 1970, Crutzen 1971). For many problems the full set of reactions may not be needed and a much shorter set can be used for the photochemical model. It should be apparent that the simplified photochemical model developed in this section may not be the most suitable one for all problems.

For the current problem we are interested primarily in the vertical distribution of ozone, the reactions which determine this distribution, and the temperature dependence of such reactions for the height range, 22-61 km. Many reactions are important in only limited height ranges. Reactions which are important only above 61 km or below 22 km are not retained. The list of reactions retained is in Table 1.

For each constituent found in Table 1 it is possible to write a continuity relation

$$\frac{dn_i}{dt} + n_i \vec{\nabla} \cdot \vec{v} = S_i - L_i \qquad (2)$$

where d/dt is the substantive derivative, $\frac{\partial}{\partial t} + \vec{v} \cdot \vec{\nabla}$, $\vec{v}$ is the velocity vector, and n_i, S_i, and L_i are the number density, source term and loss term, respectively, of the constituent i(i = $O(O(^3P))$, $O^*(O(^1D))$,

HO_2, OH, H, H_2O, H_2O_2, HNO_3, HNO_2, NO, NO_2, and NO_3). Below 70 km

$$n_i/n_m \ll 1 \tag{3}$$

where n_m is the molecular number density, so the continuity equation for n_m becomes

$$\frac{d}{dt} n_m + n_m \vec{\nabla} \cdot \vec{v} = 0. \tag{4}$$

Substituting eq (4) into eq (2) yields

$$\frac{dn_i/n_m}{dt} = (S_i - L_i)/n_m. \tag{5}$$

The ratio n_i/n_m for a constituent i is referred to as its mixing ratio.

The photochemical model now consists of 13 continuity equations of the form (5). There are several relations among the constituents which will further simplify the model. Some of these relations have been pointed out previously (Dütsch 1968, Leovy 1969a, and Crutzen 1971).

Since below 61 km less than 1% of the H_2O molecules are dissociated in a day by reactions (3) and (8), the mixing ratio of water vapor at a given height may be considered constant. Also the adjustment time for equilibrium of O* is $t(O^*) = (k_7 n_m)^{-1} < 10^{-5}$ sec and that for H is $t(H) = (n_{O_2} n_m k_{10})^{-1} < 4$ sec. Both of these

constituents may be considered in equilibrium with concentrations

$$n_{O*} \approx \frac{q_{3b} n_{O_3}}{k_7 n_m} \tag{6}$$

and

$$n_H \approx \frac{n_{OH} n_O k_9}{n_{O_2} n_m k_{10} + n_{O_3} k_{27}} . \tag{7}$$

As Leovy (1969a) indicates, eq (7) means that when reaction (27) is small compared to reaction (10), the atomic hydrogen produced in reaction (9) is destroyed so rapidly by reaction (10) that the two reactions may be replaced by the single reaction

$$OH + O \longrightarrow HO_2 \tag{8}$$

with the reaction rate, k_9. This approximation is valid below 40 km but about 5% of the hydrogen destruction at 40 km is by reaction (27) and above this height reaction (27) becomes increasingly important to the destruction of hydrogen and ozone, accounting for 20% at 60 km. Thus, if reaction rates are significantly alterred, reaction (27) could become a major one.

When the reactions involving O and O_3 are considered, it is apparent that the dominant reactions involve interconversion between O and O_3. The ratio

$$R_1 = \frac{n_O}{n_{O_3}} \approx \frac{q_{3a} + q_{3b}}{n_{O_2} n_m k_5} \tag{9}$$

has an adjustment time, $t(R_1) = (q_{3a} + q_{3b} + n_{O_2} n_m k_5)^{-1} < 10^2$ sec, which is short compared to other time scales of interest so eq (9) remains valid. Similarly the reactions involving interconversion between HO_2 and OH are dominant among those involving these two constituents. Below 40 km, where (8) may be used

$$R_2 = \frac{n_{HO_2}}{n_{OH}} \approx \frac{n_O k_9 + n_{O_3} k_{12}}{n_O k_{11} + n_{NO} k_{15}} . \tag{10}$$

which has an adjustment time of $t(R_2) = (n_O k_9 + n_{O_3} k_{12} + n_O k_{11} + n_{NO} k_{15})^{-1} < 100$ sec. Above 40 km

$$n_{OH} \approx \frac{n_{HO_2} n_O k_{11} + n_H n_{O_3} k_{27}}{n_O k_9} \tag{11}$$

and

$$n_{HO_2} \approx \frac{n_H n_{O_2} n_m k_{10} + n_{OH} n_{O_3} k_{12}}{n_O k_{11}} \tag{12}$$

which have adjustment times $t(OH) = (n_O k_9)^{-1} < 15$ sec and $t(HO_2) = (n_O k_{11})^{-1} < 15$ sec. Therefore, when eq (7) is used in eq (12) the resulting ratio is

$$R_2 = \frac{n_{HO_2}}{n_{OH}} \approx \frac{k_9}{k_{11}} \cdot \left(1 + \frac{n_{O_3} k_{27}}{n_{O_2} n_m k_{10}}\right)^{-1} . \tag{13}$$

$$+ \frac{k_{12}}{R_1 k_{11}}$$

The term $\frac{k_{12}}{R_1 k_{11}}$ in (13) becomes negligibly small above 45 km.

Finally, by similar arguments, one gets a ratio,

$$R_3 = \frac{n_{NO}}{n_{NO_2}} \approx \frac{n_O k_{16} + q_{NO_2}}{n_{O_3} k_{17}} , \tag{14}$$

which has an adjustment time $t(R_3) = (n_O k_{16} + q_{NO_2} + n_{O_3} k_{17})^{-1} < 200$ sec.

The three constituents, HNO_3, HNO_2, and NO_3 are approximately in equilibrium with values of

$$n_{HNO_3} \approx \frac{k_{19} n_m n_{NO_2} n_{OH}}{k_{21} n_O}, \tag{15}$$

$$n_{HNO_2} \approx \frac{k_{20} n_m n_{OH} n_{NO}}{k_{22} n_O}, \tag{16}$$

and

$$n_{NO_3} \approx \frac{k_{21} n_O n_{HNO_3} + k_{18} n_{NO_2} n_{O_3}}{k_{23} n_{NO}}. \tag{17}$$

Their adjustment times are: $\tau(HNO_3) = (k_{21} n_O)^{-1} < 2 \cdot 10^3$ sec, $\tau(HNO_2) = (k_{22} n_O)^{-1} < 2 \cdot 10^3$ sec and $\tau(NO_3) = (k_{23} n_{NO})^{-1} < 2 \cdot 10^3$ sec. These times may be sufficiently long for the use of equilibrium values

to be questioned. However, eqs (15), (16), and (17) permit an estimate of the densities of HNO_3, HNO_2, and NO_3 relative to the densities of NO, NO_2, HO and HO_2. These estimates indicate that the constituents HNO_3, HNO_2, and NO_3 are of minor importance in determining the vertical distribution of O_3. Therefore eqs (15), (16), and (17) are valid approximations for the present problem.

The total odd nitrogen density is the sum of the densities of NO, NO_2, NO_3, HNO_2, and HNO_3. Since the list of reactions in Table 1 does not contain sources or losses for the total odd nitrogen density, the continuity equation is

$$\frac{d}{dt}\frac{[n_{NO} + n_{NO_2} + n_{NO_3} + n_{HNO_3} + n_{HNO_2}]}{n_m} = 0 \qquad (18)$$

or, using eqs (15), (16), and (17) in eq (18), one gets

$$\frac{d}{dt}\frac{[n_{NO} + n_{NO_2}]}{n_m} = 0. \qquad (19)$$

Two sources for total odd nitrogen in the region 22-61 km are considered to be downward diffusion of NO from above 70 km where it is formed and the upward diffusion of N_2O from the troposphere, which is then destroyed by the reaction

$$N_2O + O^* \rightarrow 2NO \qquad (20)$$

with a rate $k = 9 \times 10^{-11}$ cm^3 sec^{-1} (Donovan and Husain 1970). Now the mixing ratio of N_2O is 2.5×10^{-7} at the tropopause and apparently decreases with height (Schutz et al. 1970). If we estimate the mixing ratio of $NO + NO_2$ as $10^{-9} - 10^{-7}$ (Junge 1963, Barth 1966, Pearce 1969), then the time scale for an increase in odd nitrogen density due to the two sources described is estimated to be several weeks. The possible losses to the odd nitrogen density are downward diffusion of the constituents or conversion to N_2O_5 followed by downward diffusion of that constituent.

Rather than try to include the source and loss terms for the odd nitrogen concentration, we have decided to use eq (18) or, equivalently, to set

$$(n_{NO} + n_{NO_2})/n_m = K \tag{21}$$

where K is a mixing ratio which is constant in time but a possible function of height. This highly simplified treatment of the nitrogen constituents may be justified on the grounds that we are not seeking a detailed time and height distribution for each nitrogen constituent but are trying to evaluate the importance of the nitrogen reactions to the distribution of ozone.

The constituent H_2O_2 is produced in reaction (24) and destroyed in reactions (25) and (26). The net result is the loss of HO_2 back into H_2O. This conversion also occurs in reaction (14). If reactions

(24), (25), and (26) are neglected the result is that the sum, $n_{OH} + n_{HO_2}$, calculated is too large. However, the change in the sum, $n_{OH} + n_{HO_2}$, occurring when these reactions are ignored, is significant only below 35 km. It will be shown in sections 4 and 5 that the reactions involving hydrogen are significant only above 40 km. Therefore, reactions (24), (25), and (26) are to be neglected.

The constituents O*, H, HNO_3, HNO_2, and NO_3 are considered to be in equilibrium (eqs (6), (7), (15), (16), and (17) and the water vapor mixing ratio is considered constant in time while H_2O_2 is neglected. Therefore, the continuity relations, eq (3), are needed for only the six constituents, O, O_3, NO, NO_2, HO, and HO_2. By using eqs (9), (10), and (14), the six continuity relations are reduced to three:

$$\frac{d}{dt}(1 + R_1)\varphi = C - A\varphi^2 - B\varphi\psi - F\varphi X, \tag{22}$$

$$\frac{d}{dt}(1 + R_2)\psi = D\varphi + G - E\psi^2, \tag{23}$$

and

$$\frac{d}{dt}(1 + R_3)X = 0 \tag{24}$$

where $\varphi \equiv n_{O3}/n_m$

$\psi \equiv n_{OH}/n_m$

$X \equiv n_{NO_2}/n_m$

with

$$C = 2q_2 n_{O_2}/n_m \tag{25}$$

$$A = 2R_1 k_6 n_m \tag{26}$$

$$B = (R_1 k_9 + R_1 R_2 k_{11} + k_{12}) n_m \quad z \lesssim 40 \text{ km} \tag{27}$$

$$B = \left(R_1 k_9 + R_1 R_2 k_{11} + R_1 k_9 \left(1 + \frac{n_{O_2} n_m k_{10}}{n_{O_3} k_{27}}\right)^{-1} + k_{12}\right) n_m \quad z \gtrsim 40 \text{ km} \tag{28}$$

$$F = (2R_1 k_{16} + k_{18}) n_m \tag{29}$$

$$D = 2k_8 n_{H_2O} q_{3b}/k_7 n_m \tag{30}$$

$$G = 2q_{H_2O} n_{H_2O}/n_m \tag{31}$$

$$E = 2(k_{13} + R_2 k_{14}) n_m \,. \tag{32}$$

Using (13) in (28) we get

$$B \approx 2(R_1 k_9 + k_{12}) n_m \tag{33}$$

Had we formally retained (27) above 40 km, then we would also obtain (33) as an approximation. Thus (27) may be used at all heights with only small errors. As with eq (13), k_{12} in (33) may be neglected above 45 km.

Eqs (6), (7), (9)-(17), and (22)-(32) together with the reaction rates in Table 1 comprise the photochemical model to be used in sections 3, 4, and 5.

3. ENERGY RELATION

The energy relation is

$$\rho c_v \frac{dT}{dt} = S + p \vec{\nabla} \cdot \vec{v} \tag{34}$$

where p = pressure, T = temperature, ρ = density, c_v = heat capacity at constant volume. Here

$$S \equiv \hat{E} + C \tag{35}$$

where $\hat{E}$ represents energy absorbed and C is the heat exchange due to infrared radiation. In the atmosphere the fractional pressure change is small for velocities less than that of sound (Jefferys 1930). This permits eq (34) to be approximated by

$$\frac{dT}{dt} + w \frac{g}{c_p} = \frac{1}{\rho c_p} (\hat{E} + C) \tag{36}$$

where c_p = heat capacity at constant pressure, g = gravitational constant and w is the vertical velocity. (See Ogura and Phillips, 1962, for an analysis of the validity of (31); Holton, 1971, shows that (31) is rigorously correct in a coordinate system where log p replaces z.)

As discussed in the introduction the major source of cooling in the region 22-61 km is the 15μ band of carbon dioxide. This cooling is proportional to the local blackbody function (Rodgers and Walshaw, 1966) which, for the range of temperatures found in the stratosphere,

can be approximated as a linear function of temperature. Thus, the cooling or thermal emission, is

$$\frac{1}{\rho c_p} C \approx -a(T - 180^{\circ}) \tag{37}$$

where a is a function of height. We use two different distributions of a: (1) $a = (17 \text{ days})^{-1}$ (Lindzen and Goody 1965) and (2) $a = (10 \text{ days})^{-1}$, $z > 35$ km, $a = (10 \text{ days})^{-1}\left(1 + \frac{z - 35}{20}\right)$, $z < 35$ km, (Dickinson 1968). These two distributions, referred to as slow and fast infrared cooling respectively, offer a range of cooling rates. They show the effect that changing the infrared cooling rate has on the stratospheric temperature and ozone distributions. More recently Dickinson (1972, personal communication) has suggested that 'a' continues to increase above 35 km.

The energy source may be written as

$$\hat{E} = \sum_{\ell} r_{\ell} \cdot \epsilon_{\ell} \tag{38}$$

where r_{ℓ} is the number of reactions per sec per cm^3 for reaction ℓ and ϵ_{ℓ} is the energy gain per reaction. The ϵ_{ℓ} consists of dissociation energy, D_{ℓ}, and solar energy absorbed, E_{ℓ}. With these definitions eq (33) becomes

$$\hat{E} = \sum_{\ell} r_{\ell} \ (E_{\ell} + D_{\ell}). \tag{39}$$

Solar energy absorbed by O_3, O_2, H_2O and NO_2 contributes to the source terms:

$$\sum_{\ell} r_{\ell} \; E_{\ell} = h\bar{\nu}_{O_2} q_2 n_{O_2} + h\bar{\nu}_{O_3} (q_{3a} + q_{3b}) n_{O_3}$$

$$+ h\bar{\nu}_{NO_2} q_{NO_2} n_{NO_2}$$

$$+ h\bar{\nu}_{H_2O} q_{H_2O} n_{H_2O} \tag{40}$$

where

$$q_j(z) = \int a_j I_{o\nu} \exp\left(-\sum_j a_j x_j \right) d\nu, \; j = O_2, \; O_3, \; HO_2, \; NO_2 \tag{41}$$

and

$$\nu_j = q_j^{-1} \int a_j \nu I_{o\nu} \exp\left(-\sum_j a_j x_j \right) d\nu. \tag{42}$$

Here $a_j(\nu)$ is the absorption cross section in cm^2 of the j^{th} constituent, $I_{o\nu}$ is the photon flux incident at the top of the atmosphere, x_j is the total number of molecules per cm^2 of the j^{th} constituent between the top of the atmosphere and the altitude z, h is the Planck constant and $\bar{\nu}_j$ is the mean frequency of solar photons absorbed by the j^{th} constituent. Representative variations of $(q_{3a} + q_{3b}) n_{O_3}$, $q_{O_2} n_{O_2}$, $q_{H_2O} n_{H_2O}$ and $q_{NO_2} n_{NO_2}$ with height are shown in Figure 1. It is apparent that $(q_{3a} + q_{3b}) n_{O_3} \rangle \rangle q_{O_2} n_{O_2}$ and $(q_{3a} + q_{3b}) n_{O_3} \rangle \rangle q_{H_2O} n_{H_2O}$ at all heights. Since $h\bar{\nu}_{O_3} / h\bar{\nu}_{H_2O}$ and $h\bar{\nu}_{O_3} / h\bar{\nu}_{H_2O}$ vary between 1 and 1/3, the term $h\bar{\nu}_{O_3} (q_{3a} + q_{3b}) n_{O_3}$ is much larger than $h\bar{\nu}_{H_2O} q_{H_2O} n_{H_2O}$ or $h\bar{\nu}_{O_2} q_{O_2} n_{O_2}$ at all heights. The latter two terms may be neglected

in eq (40). Above 30 km $h\bar{\nu}_{O_3}(q_{3a} + q_{3b})n_{O_3} \rangle\rangle h\bar{\nu}_{NO_2} q_{NO_2} n_{NO_2}$. Below 30 km, the ratio $(q_{3a} + q_{3b})n_{O_3}/q_{NO_2} n_{NO_2} \geq 8$, provided the mixing ratio of NO_2 does not exceed $3 \cdot 10^{-8}$ (the value used in calculating $q_{NO_2} n_{NO_2}$ for Figure 1). Since $h\bar{\nu}_{O_3}/h\bar{\nu}_{NO_2} \approx 0.7$ below 30 km, the term $h\bar{\nu}_3(q_{3a} + q_{3b})n_{O_3} \rangle h\bar{\nu}_{NO_2} q_{NO_2} n_{NO_2}$ at all heights and the latter term is neglected in eq (40). Then eq (40) becomes

$$\sum_\ell r_\ell \quad E_\ell \approx h\bar{\nu}_{O_3}(q_{3a} + q_{3b})n_m \varphi. \tag{43}$$

The second part of the energy source term in eq (39) can be written as

$$\begin{aligned}\sum_\ell r_\ell \quad D_\ell \;=\; & D(O_3)n_m \frac{dn_{O_3}/n_m}{dt} - \tfrac{1}{2}D(O_2)n_m * \left(\frac{d}{dt} n_O/n_m + \frac{d}{dt} n_{O_3}/n_m\right) \\ & + D(HO_2)n_m \frac{dn_{HO_2}/n_m}{dt} + \tfrac{1}{2}D(OH)n_m \left(\frac{dn_{OH}/n_m}{dt} - \frac{dn_{HO_2}/n_m}{dt}\right) \\ & - \tfrac{1}{2}D(H_2O)n_m \left(\frac{d}{dt} n_{HO_2}/n_m + \frac{dn_{OH}/n_m}{dt}\right) + D(NO_2)n_m \frac{d}{dt}\left(\frac{n_{NO_2}}{n_m}\right)\end{aligned} \tag{44}$$

where D(j) is the dissociation energy of the j^{th} constituent. We have evaluated (44) in detail and have found that its contribution is always small. We will mercifully spare the reader from the specifics. (N. B. (44) is identically zero for equilibrium.)

Thus eq (31) becomes

$$\frac{dT}{dz} + w\frac{g}{c_p} = \eta\phi - a(T - 180°) \tag{45}$$

where

$$\eta \equiv h\bar{\nu}_{O_3}(q_{3a} + q_{3b})n_m/\rho c_p \tag{46}$$

4. RADIATIVE-PHOTOCHEMICAL EQUILIBRIUM

The photodissociation rates and energy absorption all vary with the solar zenith angle and thus local changes in temperature and composition have a time scale of a day. The photochemical relaxation time scales are less than a day above 35 km for all constituents so calculations made with the local time changes in composition neglected should still give realistic distributions of constituents. However, the thermal relaxation time scale is a minimum of two to three days (see section 5). An estimate of the daily variation in temperature due to changing zenith angle of the sun can be made. The maximum energy absorption per day is at 50 km so the maximum daily variation in temperature would be expected at this height. At 50 km the energy absorption rate at noon is about $3 \cdot 10^{-3}$ ergs cm^{-3} sec^{-1}. Roughly one half of this energy goes to maintain the mean temperature. The noontime flux is also about half the amplitude of the diurnal oscillation in absorption. Then, from eq (45), the daily variation in temperature is estimated

$$\frac{\partial (T)_d}{\partial t} \approx \frac{(\eta\phi)_d}{\rho c_p} - a(T)_d \qquad (47)$$

where the subscript d refers to the daily variation and $a = (10 \text{ days})^{-1}$, $\rho = 10^{-6}$ g cm^{-3}, and $c_p = 10^7$ ergs $(g\ °K)^{-1}$. Thus $T_d \approx 2°K$ which is small enough that calculations made with the local temperature change neglected should still give realistic estimates of the temperature.

In the temperature relation, eq (45), the advective terms are

$$u \frac{\partial T}{\partial x} + v \frac{\partial T}{\partial y} + w \left(\frac{\partial T}{\partial z} + \frac{g}{c_p}\right) . \qquad (48)$$

The size of the winds and temperature gradients can be estimated from Leovy (1964a and 1964b), who calculated thermally driven circulations in the stratosphere and mesosphere. Between 35 and 61 km the advective terms are at least an order of magnitude less than the remaining terms. For example, at 50 km $\frac{\partial T}{\partial y} \approx 3 \cdot 10^{-3}$ °K km^{-1}, $\frac{dT}{dz} \approx 0$, $v \approx .6$ m sec^{-1}, $w \approx .08$ cm sec^{-1}, and $\frac{g}{c_p} = 10$°K km^{-1} so the vertical advective term is $\sim 8 \cdot 10^{-6}$ °K sec^{-1} and the horizontal advective term is $\sim 2 \cdot 10^{-6}$ °K sec^{-1}. Since the cooling term, $a(T - 180°)$, is $\sim 10^{-4}$ °K sec^{-1}, the advective terms can be neglected in the temperature equation. Similarly, the advective terms in the continuity equations can be neglected. For example, at 50 km the vertical scale for the ozone mixing ratio is about 24 km, so the time scale for change due to advection is $\sim 3 \cdot 10^{7}$ sec. At 50 km the ozone relaxation time is $5.4 \cdot 10^{3}$ sec so the advective terms can be neglected. Below 30 km, however, the ozone relaxation time scale increases rapidly to $3 \cdot 10^{7}$ sec while the advective time scale decreases. Therefore, below 30 km the advective terms are important in determining the ozone distribution in the atmosphere.

The possibility also exists that the tides excited by solar heating could produce mean fluxes of importance to the mean thermodynamic budget.

Careful checks indicate that this is not the case below 90 km. Thus radiative-photochemical equilibrium seems appropriate from 35-61 km.

For radiative-photochemical equilibrium eqs (22), (23), and (45) become

$$0 = C - A\varphi^2 - B\varphi\psi - FX\varphi \tag{49}$$

$$0 = D\varphi + G - E\psi^2 \tag{50}$$

$$0 = -a(T - 180^{\circ}) + \tau\varphi. \tag{51}$$

The distribution of φ, ψ, and T with height for equilibrium is found by solving eqs (49), (50), and (51) simultaneously. The solution depends on the mixing ratios of water vapor and the nitrogen oxides and on the values of the rates used for the reactions listed in Table 1.

As indicated in the preceding paragraphs these three equations are valid for the height range 35-61 km. Below this height the photochemical and thermal relaxation time scales become long enough that the neglected terms, particularly the advective terms, should be retained to find temperature and ozone distributions which agree with those observed. For convenience, eqs (49), (50) and (51) are used for the entire height range, 22-61 km, with the stipulation that the resulting radiative-photochemical equilibrium distributions are not expected to agree with those observed below 35 km.

An equilibrium solution also depends on η, q_{3a}, q_{3b}, q_{H_2C}, and q_{NO_2}, which are calculated at each height using eqs (41), (42), and (46). The spectral region, 1755-3950 Å, is divided into thirty-eight frequency intervals and the region, 4750-7000 Å, into four intervals. Below 61 km nearly all photodissociation of O_2, O_3, H_2O, and NO_2 is due to absorption of photons in these two spectral regions. Incident photon fluxes, $I_{o\nu}$, are obtained from Kondratyev (1969) for the spectral regions above 3100 Å and from Brinkmann et al. (1966) for the region below 3100 Å. It has been suggested (Hinteregger 1970) that the photon fluxes found in Brinkmann et al. (1966) for the spectral region below 1800 Å may be too large by as much as a factor of three.

Below 61 km the absorption of photons with energies corresponding

to wavelengths less than 1800 Å makes only a small contribution to dissociation rates of O_2, O_3, H_2O, and NO_2. Therefore the question of the magnitude of photon fluxes for the spectral region below 1800 Å is not important for our calculations.

Actual cross sections, a_j, for absorption by the j^{th} constituent vary with frequency. For each frequency interval the average cross section, $\bar{a}_j$, was used. Cross sections for O_3 are from Griggs (1968) and Inn and Tanaka (1953). Those for H_2O are from Watanabe and Zelikoff (1953) and Thompson et al. (1963). Those for NO_2 are from Hall and Blacet (1952) and Nakayama et al. (1959). It is more difficult to determine the appropriate cross section for O_2 in a given frequency interval due to the presence of the Schumann-Runge absorption band which has numerous narrow rotation lines. One way of treating the absorption in the Schumann-Runge band is to consider the absorption cross section for O_2 as a function of both frequency and path length (Hudson et al. 1969). Then it is possible to divide the atmosphere in layers vertically and calculate the absorption coefficient of a given frequency interval for each layer (Brinkmann 1969). The atmosphere between 61 and 22 km is divided into twenty-four layers.

The water vapor mixing ratio is not well determined in the stratosphere. Some observations (Mastenbrook 1968, Schölz 1970) indicate a value of $2 \cdot 10^{-6}$ - $3 \cdot 10^{-6}$ at 29 km and $2 \cdot 10^{-6}$ - $6 \cdot 10^{-6}$ at 50 km. The value of the mixing ratio used at a given height is

important at lower heights only if water vapor is a significant absorber of solar photons or if the hydrogen reactions strongly affect the ozone density since ozone is a strong absorber of solar energy. In the height range 22-61 km the attenuation of incoming solar radiation due to absorption by water vapor is negligible. It is found that hydrogen reactions are dominant in determining the ozone density above 40 km for a water vapor mixing ratio of $5 \cdot 10^{-6}$. The height above which the hydrogen reactions are dominant increases with decreasing water vapor mixing ratio. Since attenuation of solar energy by ozone is small above 50 km, it is only at heights below this that the vertical distribution of water vapor above is important. The effect of varying the mixing ratio of water vapor with height is not investigated here. For convenience the mixing ratio for water vapor is assumed to be constant with height and is varied from 0, 10^{-8}, 10^{-7}, 10^{-6}, $5 \cdot 10^{-6}$ to 10^{-5} for successive cases. By this variation we show the importance of water vapor in determining the vertical distributions of ozone and hence temperature.

As indicated in section 2, the vertical distribution for the mixing ratio of the nitrogen oxides, NO and NO_2, is not well known. However, if downward diffusion of NO from above 70 km occurs, the mixing ratio of NO must increase with height. The mixing ratio of nitrogen oxides, K, is defined in eq (21), and may be written, by use of eq (14), as

$$K = (1 + R_3)X. \tag{52}$$

K is given two different distributions:

$$\begin{aligned} &(1)\ K = 3\cdot10^{-8}\exp(z-35)/H && z \rangle 35 \text{ km} \\ &\qquad = 3\cdot10^{-8} && z \langle 35 \text{ km} \end{aligned} \tag{53a}$$

and

$$\begin{aligned} &(2)\ K = 3\cdot10^{-9}\exp(z-35)/H && z \rangle 35 \text{ km} \\ &\qquad = 3\cdot10^{-9} && z \langle 35 \text{ km} \end{aligned} \tag{53b}$$

where H = 9.25 km. These two distributions are within the range of observations discussed in section 2. They should be helpful in determining the importance of the nitrogen reactions to the ozone and temperature distributions. The terms, high nitrogen and low nitrogen, refer to distributions (1) and (2), respectively.

Reaction rates (5)-(26) are uncertain. Three different sets of rates are used for reactions (5) and (6) (the pure oxygen reactions) and these three sets are listed in Table 2. The rates to use for reactions (7)-(26) are individually increased or decreased by a factor of 10 and the equilibrium distributions of constituents and temperatures are recalculated. It should be noted that the rates for reactions involving HNO_2 are not known. It is assumed that these rates are the same as those for similar reactions involving HNO_3. This assumption is admittedly a guess which permits an estimate of the number density of HNO_2. From eq (16) it is found that the number density of HNO_2, is sufficiently small that the equilibrium estimate of HNO_2 by eq (16) is adequate for the current work. Even if the actual rates for reactions (20) and (22) are such as to increase the number density of HNO_2 by two orders of magnitude from those estimated in eq (16) using

the rates in Table 1, the effect of HNO_2 in the current work could still be treated by use of eq (16). Since reactions (20) and (22) do not appear in eqs (49), (50), and (51), the rates used for these reactions will not invalidate the calculated temperatures or concentrations unless the actual rates are such that the number density of HNO_2 is more than two orders of magnitude larger than estimated. If the actual rates are such that HNO_2 number density is more than two orders of magnitude larger than estimated here, the validity of eq (16) would have to be reconsidered.

In solving eqs (49), (50), and (51) consideration must be given to the fact that the thermal emission, as represented in eq (51) by $-a(T - 180°)$, occurs twenty-four hours a day while the absorption of solar energy and photochemistry as given by the other terms in the three equations, occur only during the daylight hours. Therefore, in eqs (49), (50), and (51) the terms involving either absorption of solar energy or photochemistry are calculated for their noontime values at the solar equinox and then these values are divided by two. Above 50 km where absorption does not vary much over the daylight hours, this approximation is fair. However, at lower altitudes it obviously overestimates absorption. That this is the case is shown in time dependent calculations which we will mention later; the average temperatures obtained from time dependent calculations are generally 10-15°C less than the equilibria calculated here. The thermal emission term is used at its full value because it operates the entire day. Since the rate of

absorption of solar energy at a given height is also a function of latitude, equilibrium calculations are made at two latitudes: 0° and 45°.

In Figures 2 and 3 (0° latitude) and Figures 4 and 5 (45° latitude) are shown the radiative-photochemical distributions of temperature and ozone density for six cases: (1) O (hydrogen and nitrogen reactions neglected), (2) H + O (nitrogen reactions neglected), (3) N + O (low) (hydrogen reactions neglected), (4) N + O (high) (hydrogen reactions neglected), (5) N + H + O (low), and (6) N + H + O (high). For all six cases the rates in set 1 (Table 2) are used for reactions (5) and (6), and the fast vertical distribution for a. When the hydrogen reactions are included, we use the $5 \cdot 10^{-6}$ ratio for water vapor.

Differences among the six different cases are most striking in the temperature profile (Figures 2 and 4). The O case shows a linear increase in temperature up to 45 km and then a very small decrease in temperature above. The inclusion of the nitrogen reactions (low mixing ratio for nitrogen oxides) decreases the equilibrium temperature and ozone density below 30 km and has little effect on the distributions above 30 km. The effect of the nitrogen reactions is more pronounced when the high mixing ratio of nitrogen oxides is used. The temperature below 50 km is considerably reduced ($\sim 20^{\circ}$K) from the pure O case and the ozone density below 40 km is also considerably reduced ($\sim 40\%$).

Inclusion of the hydrogen reactions has little effect below 40 km but above this height strongly reduces the ozone density and temperature from the values found for the pure O case. When the hydrogen reactions are included, they are dominant in determining the temperature and ozone density above 45 km even when the nitrogen reactions are also included with either the low or high mixing ratio for nitrogen oxides. Most significantly, there appears to be no way of producing a temperature decrease of the observed magnitude above the stratopause without including hydrogen reactions!

Water vapor must be dissociated before the resultant constituents H, OH, and HO_2, can act by means of the hydrogen reactions to reduce ozone density and thus temperature. It might be expected, since the mixing ratio of water vapor is assumed constant with height, that the hydrogen reactions would be important at all heights, not just above 40 km. However, the dissociation of water vapor is strongly height-dependent. The photodissociation of water vapor below 61 km is due to absorption of solar radiation with energies corresponding to wavelengths below 2000 Å, which is strongly attenuated below 85 km due to absorption by O_2 and O_3. As a result q_{H_2O} decreases from $4.3 \cdot 10^{-8}$ sec^{-1} at 61 km to $1.1 \cdot 10^{-11}$ sec^{-1} at 22.5 km. Water vapor is also dissociated in reaction (8) and the rate of dissociation depends on the density of O*. From eq (6) the density of O* is proportional to q_{3b}

which is the absorption rate of radiation by ozone below 3100 Å. The radiation below 3100 Å is significantly attenuated below 45 km and q_{3b} decreases from $8 \cdot 10^{-3}$ sec^{-1} at 45 km to $1.1 \cdot 10^{-4}$ sec^{-1} at 22.5 km. It is apparent that the dissociation of water vapor increases with height and, as a result, the hydrogen reactions are more important to equilibrium distribution of ozone density and temperature with increasing height.

In Figure 6 equilibrium temperature profiles are shown for the three different sets of rates for reactions (5) and (6) and for the two cooling rate coefficients, fast and slow. The water vapor mixing ratio used is $5 \cdot 10^{-6}$ while the low mixing ratio for nitrogen oxides is used. The slow cooling rate coefficient (a^{-1} = 17 days) is 70% longer than the fast one (a^{-1} = 10 days) above 35 km. From eq (50) it might be expected that a 70% decrease in 'a' would lead to a 70% increase in (T-180°) rather than the 25% increase (at 45 km) indicated in Figure 6. Such is not the case, since the ozone density itself is strongly temperature dependent through reactions (5) and (6) and increasing the temperature decreases the ozone density and thus the absorption of energy. Therefore the equilibrium temperature is buffered against change. An alteration in the cooling is nearly compensated for by a corresponding alteration in the heating so the fractional change in the equilibrium temperature is actually much smaller than the fractional changes in either the cooling or heating.

Coupling of temperature and ozone density is obvious for an O atmosphere (neglecting the hydrogen and nitrogen reactions) since (49) becomes

$$O = C - A\varphi^2 \tag{54}$$

and, from eqs (26) and (9)

$$A = \frac{2(q_{3a} + q_{3b})k_6}{n_{O_2} k_5}$$

in which the ratio k_6/k_5 is strongly temperature dependent. It should be noted that for each set of rates for k_5 and k_6 in Table 2, the ratio k_6/k_5 is strongly temperature dependent. In fact, the temperature dependence of k_6/k_5 for set 1 is exp (-3395/T) which is very close to that of exp (-3295/T) found for set 2. The temperature dependence of set 3 is somewhat less and the effect of this will be discussed in section 5. When hydrogen reactions are dominant in determining the ozone density (as appears to be the case above 45 km for a water vapor mixing ratio of $5 \cdot 10^{-6}$) it might appear that the temperature dependence of the ozone density would be greatly reduced, since the hydrogen reactions do not have rates that are strongly temperature dependent. Above 45 km eq (49) can be approximated, by use of eqs (27) and (9), as

$$O = C - B\phi\psi \tag{55}$$

where (above 45 km),

$$B \cong \frac{2(q_{3a} + q_{3b})k_9}{n_{O_2} k_5} . \tag{56}$$

It is true that k_9 is not temperature dependent but k_5 is strongly temperature dependent. Therefore, the presence of hydrogen reactions does not eliminate the buffering of the temperature profile. This result should be expected since the hydrogen reactions only destroy ozone while the production of ozone by reaction (5) is temperature dependent no matter what destruction processes are dominant. Eqs (55) and (56) indicate that the ozone density and, thus, temperature profile above 45 km are dependent on the rate used for reaction (5). The temperature profiles in Figure 6, where three different values are used for the rate of reaction (5), show this dependence.

The mixing ratio of OH may be estimated from eq (50) as

$$\psi = \left(\frac{D\varphi + G}{E}\right)^{1/2} . \tag{57}$$

The use of eqs (30), (31), and (32) in (57) gives

$$\psi = \left\{\frac{k_8 q_{3b} \varphi / k_7 + q_{H_2O}}{(k_{13} + R_2 k_{14}) n_m}\right\}^{1/2} \left\{\frac{n_{H_2O}}{n_m}\right\}^{1/2} . \tag{58}$$

Thus the mixing ratio of OH is proportional to the square root of the water vapor mixing ratio. From eq (49) it is apparent that the importance of the hydrogen reactions to the ozone mixing ratio is directly proportional to $B\phi\psi$. Thus, increasing the water vapor mixing ratio both increases the importance of the hydrogen reactions at a given height and decreases the height at which the hydrogen reactions become dominant in determining the ozone mixing ratio.

Above 45 km eq (13) may be used for R_2; i.e.,

$$R_2 \approx \frac{k_9}{k_{11}} \left(1 + \frac{n_{O_3} k_{27}}{n_{O_2} n_m k_{10}}\right)^{-1} \tag{59}$$

and (58) becomes

$$\psi \approx \left\{ \frac{(k_8 q_{3b} \phi / k_7 + q_{H_2O}) k_{11}}{k_9 k_{14} n_m \left(1 + \frac{n_{O_3} k_{27}}{n_{O_2} n_m k_{10}}\right)^{-1}} \right\}^{1/2} \left(\frac{n_{H_2O}}{n_m}\right)^{1/2} . \tag{60}$$

Also, above 45 km, we may use an approximate form of (33); i.e.,

$$B \approx 2R_1 k_9 n_m \tag{61}$$

Eqs (59), (60), and (61) are not used in our radiative photochemical equilibrium calculations but they are useful in estimating the effect of varying the rates for the hydrogen reactions.

It is apparent from eq (60) that changes in k_8, k_{11}, k_9, k_{14}, k_{27}, and k_{10} will be undistinguishable in their effects from changes in the assumed water vapor mixing ratio. The effect of varying the water vapor mixing ratio has been discussed previously. We shall return to this matter later in evaluating our quantitative results.

The effect of the nitrogen reactions on the ozone mixing ratio is indicated in eq (49) by $- F\phi X$. Use of eqs (28), (14), and (21) plus the fact that $R_1 k_{16} > k_{18}$ at all heights yields

$$F\varphi X \approx \frac{2R_1 k_{16} n_m K\varphi}{1 + R_3} \tag{62}$$

Using eq (14) we estimate that $R_3 < 1$ below 35 km and $R_3 \approx R_1 k_{16}/k_{17}$ above 35 km so

$$F\varphi X \approx 2R_1 k_{16} n_m K\varphi \text{ below 35 km} \tag{63}$$

and

$$F\varphi X \approx 2R_1 k_{16} n_m K\varphi/(1 + R_1 k_{16}/k_{17}) \text{ above 35 km} \tag{64}$$

It is apparent from eqs (63) and (64) that variations in k_{16} or k_{17} may be equivalently expressed as changes in K, the mixing ratio of nitrogen oxides. The effect on the ozone mixing ratio due to varying the nitrogen oxides mixing ratio has already been indicated.

Finally, it should be noted that below 30 km the photochemical time scale for ozone is so long (several weeks to years) that dynamical effects can be significant. It follows that joint radiative-photochemical equilibrium calculations should not be expected to give results in agreement with observed temperature and ozone density distributions. Above 35 km both the photochemical time scale (< 1 day) and the radiative-photochemical cooling time scale (about a few days) are short enough that dynamical effects are unimportant. Therefore equilibrium calculations should give appropriate values of ozone density and temperature.

Figures 2-6 clearly show that distributions of ozone temperature and density depend on values used for parameters such as reaction rates, cooling time scale, and mixing ratios of water vapor and nitrogen oxides. These parameters can be adjusted to yield distributions which best match the observed distributions of ozone density and temperature. Comparison of ozone measurements made by several investigators (Johnson et al. 1954, Rawcliffe et al. 1963, Miller and Stewart 1965, Weeks and Smith 1968, Hilsenrath et al. 1969) shows a range in number density as large as an order of magnitude at some heights in the 35-61 km region. Since the temperature in this region is much better determined as in the U. S. Standard Atmosphere 1962 or Supplemental Atmospheres (Handbook of Geophysics and Space Environments), temperature rather than

ozone density is used to determine the match of the equilibrium calculations to observations. However, as we shall see, a rather systematic difference between our predicted ozone distribution and those observed may indicate an error in our choice of cooling rate coefficient.

The Supplemental Atmosphere (Tropical) has a stratopause temperature of 270°K with 243°K at 35 km and 250°K at 61 km. In Figures 2, 4, and 6 all stratopause temperatures are higher than 270°K. Of the three sets of reaction rates for the pure oxygen reactions, set 1 gives the smallest st ratopause temperature. Also, from Figure 6 the fast cooling rate ($a = (10 \text{ days})^{-1}$ above 35 km) always gives lower stratopause temperatures than the slow cooling rate ($a = (17 \text{ days})^{-1}$). Set 1 for the pure oxygen reaction rates and the fast cooling rate are used in the calculations to model the temperature. This choice means smaller mixing ratios of water vapor and nitrogen oxides are needed to lower the calculated stratopause temperature to that of the Supplemental Atmosphere (Tropical) than if a slower cooling rate or another set of rates for the pure oxygen reactions were used.

Temperature profiles in Figures 2 and 4 indicate that cases with water vapor absent have a nearly constant temperature above the stratopause while cases with a water vapor mixing ratio of $5 \cdot 10^{-6}$ show a decrease of 55-75°K in temperature from the stratopause to 61 km. Since the Supplemental Atmosphere (Tropical) has a 20°K decrease from

the stratopause to 61 km, the water vapor mixing ratio is between zero and $5 \cdot 10^{-6}$. A value of $5 \cdot 10^{-7}$ gives $\sim 23^{\circ}$K decrease between the stratopause and 61 km but is less than the $2\text{-}6 \cdot 10^{-6}$ value for the water vapor mixing ratio that measurements indicate (Mastenbrook 1968, Schölz et al. 1970). As eqs (60) and (61) indicate a decrease in the dissociation rates of water vapor, a decrease in k_{11} or k_9, or an increase in k_{14} would mean the water vapor mixing ratio must be increased to maintain the same calculated equilibrium temperature profile.

The effect of various nitrogen oxide mixing ratios on the stratopause temperature is shown in Table 3. Profiles 1 and 2 are the low and high nitric oxide mixing ratios described previously. Profiles 3, 4, and 5 have constant nitrogen oxides mixing ratios of $K = 3 \cdot 10^{-9}$, $3 \cdot 10^{-8}$, and $1 \cdot 10^{-7}$, respectively. Profile 6 has

$$K = 3 \cdot 10^{-9} \qquad z < 35 \text{ km}$$

$$K = 3 \cdot 10^{-9} \exp\left(\frac{z - 35}{6}\right) \qquad 35 \text{ km} < z < 45 \text{ km}$$

$$K = 1.6 \cdot 10^{-8} \qquad z > 45 \text{ km}.$$

Profile 7 is simply Profile 6 with the K values multiplied by 10. Profile 8 has no nitrogen oxides included. Profiles 2, 5, and 7 yield about the same stratopause temperature. Profile 5 with a constant mixing ratio is unsuitable since the temperature decreases by 56°K from the

stratopause down to 35 km as opposed to a 27°K decrease in the Supplemental Atmosphere (Tropical). Profile 2 has a mixing ratio of nitrogen oxides which continues to increase with height above 45 km. Consequently the temperature decrease from the stratopause to 61 km is 31°K for Profile 2 as opposed to 23°K for Profile 7 which has a constant nitrogen oxides mixing ratio above 45 km. Therefore Profile 7 is preferred of those tried. The mixing ratio of nitrogen oxides at a given height affects the calculations at lower heights only if the amount of solar energy reaching the lower heights depends on the nitrogen oxides mixing ratio higher up. This dependence occurs if the nitrogen oxides are strong absorbers of solar energy or if the nitrogen reactions strongly alter the ozone density since ozone is a strong absorber of solar energy in the relevant frequency intervals. The former is not true and above 50 km, for the mixing ratios of nitrogen oxides used here, neither is the latter. Thus, equilibrium distributions found at the stratopause depend only on the nitrogen oxides mixing ratio at that height. From Table 3, we conclude that, since Profiles 2, 5, and 7 all give stratopause temperatures of about the same size, that a mixing ratio for nitrogen oxides in the range of $8\text{-}16 \cdot 10^{-8}$ is acceptable for the reaction and cooling rates used. However, as will be seen in section 6a, our choice of cooling rate may be too low in which case we are requiring that ozone density be too low and consequently exaggerating the need for ozone loss processes. A larger value of 'a' will much diminish our need for NO_x. Moreover, we are really specifying FX in

(49) rather than the NO_x mixing ratio, and changes in reaction rates would alter our estimate for the latter.

From eq (64) it is apparent that the mixing ratio of nitrogen oxides needed to give a particular temperature distribution is altered when the reaction rates, k_{16} and k_{17}, are altered.

The treatment of the day-night differences in photochemistry is fairly crude. However, time-dependent calculations have been made for the daily variations in ozone density and temperature for Profiles 7 and 8. The temperatures at the stratopause, averaged over 24 hours, are listed in Table 3. The stratopause temperature from the time-dependent calculations is 15°- 17°K lower than that found in the joint radiative-photochemical equilibrium calculations. For Profile 7 the resulting stratopause temperature of 273°K is in good agreement with the 270°K stratopause temperature of the Supplemental Atmosphere (Tropical). The results of the time-dependent calculations will be reported separately.

The 15°K difference between stratopause temperature found for radiative-photochemical equilibrium calculations and for the time-dependent calculations when the same reaction rates and mixing ratios of water vapor and nitrogen oxides are used is due to the crude averaging technique for day-night differences in the radiative-photochemical calculations. As discussed earlier in this section solar energy absorption occurs only during daylight hours. The average energy absorption

rate was set equal to half of the noontime energy absorption rate. It was pointed out that this treatment of day-night differences leads to an overestimate in the energy absorption rate and, consequently, an overestimate in the radiative-photochemical temperature. From eqs (49), (50), (51), (55), and (56) it is seen that a stratopause temperature of 273°K instead of 288°K results when (all other parameters being the same) the noontime energy absorption divided by 2.4 instead of 2 is used for the average energy absorption rate.

4a. CRITICAL ASSESSMENT OF EQUILIBRIUM RESULTS

The above results while interesting are not as important as the fact that the system we have developed is simple enough to permit the immediate evaluation of the effects of various changes and the identification of questionable rate coefficients. In this section we will use this simplicity in order to assess and extend the results obtained above.

In the above scheme we have essentially asked what amount of ozone is necessary to produce the observed mean temperature between 35 km and 60 km. The amount is less than what one would obtain from simple oxygen chemistry. So we further inquired how much H_2O and NO_x would be needed for the various catalytic destructions of ozone to reduce the value to that needed. For the reaction and cooling rate coefficients used we obtained answers to these questions, and these answers seem questionable on at least three counts:

i) The density of ozone calculated between 40 and 50 km is about 30% less than the few existing measurements indicate;

ii) The suggested mixing ratio for NO_x at 50 km, $1.6 \cdot 10^{-7}$, is higher than has hitherto been suggested; and

iii) The mixing ratio for H_2O suggested, $5 \cdot 10^{-7}$, is less than currently believed.

For argument's sake, let us assume the above discrepancies are are real, and attempt to track down their origins. Item (i) is entirely determined by eq (51); i.e., it is independent of any chemical assumptions, and depends only on our choice of solar intensity and absorption cross-sections in ozone's absorption bands and on our choice of 'a', the cooling rate coefficient. Considerable uncertainty exists concerning the value of 'a' at 50 km. If it were 30% larger, 30% more ozone would be needed to produce the observed $\bar{T}$. Dickinson (1972, private communication) has informed us that his current calculations of 15μ CO_2 cooling suggest that 'a' indeed continues to increase above 35 km to values on the order of 30% higher than 1/10 days above 40 km.

With 30% more ozone above 40 km, the loss terms due to hydrogen and nitrogen reactions must be reduced. Assuming our reaction rates are correct, this can be achieved by reducing our mixing ratios for NO_x and H_2O. We rule out the latter on two counts:

a) Our value for n_{H_2O}/n_m already seems low (viz item 3), and, more important,

b) The value we have chosen for n_{H_2O}/n_m determines not only the value of ϕ (and hence temperature) at 50 km but also the gradient of temperature above 50 km where NO_x has a negligible effect.

We are, therefore, forced to reduce our mixing ratio for NO_x. To allow for 30% more ozone, this mixing ratio must be decreased from $1.6 \cdot 10^{-7}$ to about $2.4 \cdot 10^{-8}$. The latter value seems more plausible (viz item (ii)) and in turn supports the choice of the larger value for 'a'. Thus, a plausible choice for the NO_x mixing ratio between 35 and 50 km appears to be $2\text{-}3 \cdot 10^{-8}$. This is considerably more (by about a factor of 20) than what is expected will be produced by full scale SST operations (Johnston, 1972). Thus, while SST effects should be discernible, they should not be catastrophic. In particular, a change of 5% in NO_x should not produce a similar change in ϕ since nitrogen reactions are not the only loss processes for ozone and also because of the thermal buffering already described. Turning, finally, to item (iii) we must note that the quantity we have chosen is not really n_{H_2O}/n_m but $B\psi$ in eq (49). From eqs (60) and (61) we have that

$$B\psi \approx \frac{2(q_{3a} + q_{3b})k_9}{n_{O_2} k_5} \left\{ \frac{(k_8 q_{3b} \phi / k_7 + q_{H_2O})k_{11}}{k_9 k_{14} n_m \left(1 + \dfrac{n_{O_3} k_{27}}{n_{O_2} n_m k_{10}}\right)^{-1}} \right\}^{1/2} \left(\frac{n_{H_2O}}{n_m}\right)^{1/2}$$

above 45 km.

Clearly, various changes in reaction rate coefficients could allow a greater value for $\left(\frac{n_{H_2O}}{n_m}\right)$ without changing $B\psi$. Recent measurements brought to our attention by S. Wofsy suggest our rate for k_8 should be increased from $5 \cdot 10^{-11}$ to $2 \cdot 10^{-10}$ while k_{14} should be changed from

10^{-11} to $2 \cdot 10^{-10}$ (see Wofsy et al. 1972 for references). With these new rates $\frac{n_{H_2O}}{n_m}$ must be increased to about $3 \cdot 10^{-6}$ to maintain a given value for $B\psi$. Discrepancy (iii) argues in favor of the new rates.

5. RELAXATION TIME SCALES

Suppose we consider small perturbations from the radiative-photochemical equilibrium state calculated in section 4. Then linearization of eqs (22), (23), and (45) yields the equations which can be solved for the time scales for return to radiative-photochemical equilibrium. The equations are, with winds neglected,

$$\frac{\partial \varphi'}{\partial t} = -\mathcal{B}\,\varphi' - C\psi' - \mathcal{Y}\,T', \tag{65}$$

$$\frac{\partial \psi'}{\partial t} = \mathcal{D}\,\varphi - \mathcal{E}\,\psi' - \mathcal{F}\,T', \tag{66}$$

$$\frac{\partial T'}{\partial t} = \eta\varphi' - aT' \tag{67}$$

where, using primes for perturbation quantities and overbars for equilibrium value,

$$\varphi = \bar{\varphi} + \varphi',$$

$$\psi = \bar{\psi} + \psi',$$

$$T = \bar{T} + T',$$

$$\frac{n_m'}{\bar{n}_m} \approx -\frac{T'}{\bar{T}} \text{ (valid for small pressure perturbations)}$$

$$\mathcal{B} = [2\bar{A}\bar{\varphi} + \bar{B}\bar{\psi}(1 + \delta_1) + \bar{F}\bar{X}(1 + \epsilon_1)]/(1 + R_1), \tag{68}$$

$$C = \bar{B}\bar{\varphi}/(1 + R_1), \tag{69}$$

$$\mathcal{U} = \frac{\bar{\varphi}}{\bar{T}}[\alpha\bar{A}\bar{\varphi} + (\beta - \delta_2\epsilon_2)\bar{B}\bar{\psi} + (f + \epsilon_2)\bar{F}\bar{X}]/(1 + R_1), \tag{70}$$

$$\mathcal{D} = [\bar{D} - g\bar{E}\bar{\psi}^2/\bar{\varphi}]/(1 + R_2), \tag{71}$$

$$\mathcal{E} = 2\bar{E}\bar{\psi}/(1 + R_2), \tag{72}$$

and

$$\mathcal{F} = [r\bar{E}\bar{\psi}^2/\bar{T}]/(1 + R_2) . \tag{73}$$

Further definitions are

$$\alpha = 1 + e_6 - e_5,$$

$$\gamma_4 = \gamma_1 + \gamma_2,$$

$$\gamma_1 = \frac{k_{16}k_{15}}{k_{17}\bar{\varphi}}\bar{X}/[k_{11} + \frac{R_3\bar{X}k_{15}}{R_1\bar{\varphi}}],$$

$$\gamma_2 = \frac{k_{15}\bar{X}q_{NO_2}}{R_1\bar{\varphi}^2\bar{n}_m k_{17}}/[k_{11} + \frac{R_3\bar{X}k_{15}}{R_1\bar{\varphi}}],$$

$$\omega = \frac{k_{12}}{k_{12} + R_1k_9}[e_{12} - (2 - e_5)] - \gamma_1(e_{15} + e_{16} - e_{17})$$

$$- \gamma_2[e_{15} + 1 - e_{17} - (2 - e_5)],$$

$$\epsilon_1 = q_{NO_2}/[(1 + R_3)(\bar{\varphi}\bar{n}_m k_{17})],$$

$$\epsilon_2 = -\frac{R_1 k_{16}}{(1 + R_3)k_{17}}[e_{16} + (2 - e_5) - e_{17}] - \epsilon_1(1 - e_{17}),$$

$$g = \gamma_3 \qquad z \le 40 \text{ km}$$

$$g = -\Delta/(1 + \Delta)^2 \cdot \frac{k_9}{k_{11}} \frac{1}{R_2} \qquad z \ge 40 \text{ km}$$

$$\Delta = \bar{\phi} \frac{k_{27}}{n_{O_2} k_{10}}$$

$$\gamma_3 = \gamma_4(1 + \epsilon_1/R_3)$$

$$r = \omega - \epsilon_2\gamma_4 - 1 \qquad z \le 40 \text{ km}$$

$$= -\frac{\Delta}{(1 + \Delta)^2} \cdot \frac{k_9}{k_{11}R_2}(e_{27} + 1) + \frac{k_{12}}{R_1 k_{11} R_2}(e_{12} - 2 + e_5) - i$$

$$z \ge 40 \text{ km}$$

$$f = -1 + [2R_1 k_{16}(e_{16} + 2 - e_5) + k_{18}e_{18}]/[2R_1 k_{16} + k_{18}]$$

$$\beta = -1 + [(k_9 + R_2 k_{11})(2 - e_5)R_1 + R_1 R_2 R_{11}\omega + k_{12}e_{12}]n_m/\bar{B}$$

$$\delta_1 = \gamma_3 R_1 R_2 k_{11} n_m / \bar{B}$$

$$\delta_2 = \delta_1 \gamma_4 / \gamma_3$$

$$e_i = \frac{\bar{T}}{k_i}\left(\frac{dk_i}{dT}\right)_{\bar{T}} \qquad (i = 5, 18),$$

and, from the linearization of eq (24),

$$\frac{X'}{\bar{X}} = \epsilon_1 \frac{\varphi'}{\bar{\varphi}} + \epsilon_2 \frac{T'}{\bar{T}} .$$

The complexity of our coefficients in (65) and (66) arises because some of the reaction rates, k_i, and the ratios R_1, R_2, and R_3 are temperature dependent and the ratios R_2 and R_3 are also dependent on the ozone mixing ratio. There are additional terms in eqs (65) and (66) which have been neglected since they are much smaller than those retained. If there is no coupling, then the time scale for return to equilibrium is $\mathcal{B}^{-1}$ for the ozone mixing ratio, $\mathcal{E}^{-1}$ for the hydroxyl mixing ratio, and a^{-1} for the temperature. The terms $C\psi'$, $\mathcal{A}\,T'$, $\mathcal{D}\,\phi'$, $\mathcal{F}T'$, and $\eta\phi'$, represent the coupling between the photochemical and radiative processes.

Eqs (65), (66), and (67) may be combined to:

$$\left[\frac{\partial^3}{\partial t^3} + M\frac{\partial^2}{\partial t^2} + N\frac{\partial}{\partial t} + S\right]\begin{Bmatrix}\varphi' \\ \psi' \\ T'\end{Bmatrix} = 0 \tag{74}$$

where

$$M = a + \mathcal{B} + \mathcal{E}$$

$$N = \mathcal{B}\mathcal{E} + a\mathcal{B} + \mathcal{E}a + \mathcal{H}_\eta + C\mathcal{D}$$

$$S = \mathcal{E}a\mathcal{B} + \eta\mathcal{H}\mathcal{E} + Ca\mathcal{D} - \mathcal{F}C_\eta .$$

Initial conditions are needed to solve eq (74) and we consider three cases:

(1) $\varphi'(t = 0) = \varphi(0)$,

$\psi'(t = 0) = 0$,

$T'(t = 0) = 0$,

(2) $\varphi'(t = 0) = 0$,

$\psi'(t = 0) = \psi(0)$,

$T'(t = 0) = 0$,

and (3) $\varphi'(t = 0) = 0$,

$\psi'(t = 0) = 0$,

$T'(t = 0) = T(0)$.

The solution for φ' for case 1 is

$$\varphi' = \varphi(0)\ K_{11}e^{\sigma_1 t} + K_{21}e^{\sigma_2 t} + K_{31}e^{\sigma_3 t};$$

the solution for ψ' for case 2 is

$$\psi' = \psi(0)\ K_{12}e^{\sigma_1 t} + K_{22}e^{\sigma_2 t} + K_{32}e^{\sigma_3 t}.$$

and the solution for T' for case 3 is

$$T' = T(0)\ K_{13}e^{\sigma_1 t} + K_{23}e^{\sigma_3 t} + K_{33}e^{\sigma_3 t}.$$

The coefficients are defined as

$$K_{1j} = (\theta_j + V_j(\sigma_2 + \sigma_3) + \sigma_2\sigma_3)/[(\sigma_1 - \sigma_3)(\sigma_1 - \sigma_2)];$$
$$K_{2j} = (\theta_j + V_j(\sigma_3 + \sigma_1) + \sigma_1\sigma_3)/[(\sigma_2 - \sigma_3)(\sigma_2 - \sigma_1)];$$
$$K_{3j} = (\theta_j + V_j(\sigma_1 + \sigma_2) + \sigma_1\sigma_2)/[(\sigma_3 - \sigma_1)(\sigma_3 - \sigma_2)]$$

where j = 1, 2, 3 and

$$V_1 = \mathcal{B},$$
$$V_2 = \mathcal{E},$$
$$V_3 = \mathcal{a},$$
$$\theta_1 = \mathcal{B}^2 - \eta\mathcal{E} - C\mathcal{D},$$
$$\theta_2 = \mathcal{E}^2 - C\mathcal{D},$$
$$\theta_3 = \mathcal{a}^2 - \eta\mathcal{D}.$$

The values σ_1, σ_2, and σ_3 are roots of the cubic equation:

$$\sigma_3 + M\sigma^2 + N\sigma + S = 0 \qquad (75)$$

which follows from eq (74).

For cases where the hydrogen reactions are neglected (74) reduces to:

$$\left[\frac{\partial^2}{\partial t^2} + (a + \mathcal{B})\frac{\partial}{\partial t} + (a\mathcal{B} + \mathcal{J}\eta)\right]\left(\frac{\varphi'}{T'}\right) = 0 \qquad (76)$$

with the solution for φ' (case 1) as

$$\varphi' = \varphi(0)\left[\frac{\hat{\sigma}_2 + \mathcal{B}}{\hat{\sigma}_2 - \hat{\sigma}_1} e^{\hat{\sigma}_1 t} - \frac{\hat{\sigma}_1 + \mathcal{B}}{\hat{\sigma}_2 - \hat{\sigma}_1} e^{\hat{\sigma}_2 t}\right] \qquad (77)$$

and the solution for T' (case 3) as

$$T' = T(0)\left[\frac{\hat{\sigma}_2 + \alpha}{\hat{\sigma}_2 - \hat{\sigma}_1} e^{\hat{\sigma}_1 t} - \frac{\hat{\sigma}_1 + \alpha}{\hat{\sigma}_2 - \hat{\sigma}_1} e^{\hat{\sigma}_2 t}\right] \qquad (78)$$

where

$$\hat{\sigma}_1 = \frac{1}{2} - (a + \mathcal{B}) - \left[(a - \mathcal{B})^2 - 4\eta\mathcal{J}\right]^{1/2} \qquad (79)$$

$$\hat{\sigma}_2 = \frac{1}{2} - (a + \mathcal{B}) + \left[(a - \mathcal{B})^2 - 4\eta\mathcal{J}\right]^{1/2}. \qquad (80)$$

In Figure 7 time scales a^{-1}, $\mathcal{B}^{-1}$, $\tau_1 (= -(\mathrm{Re}\hat{\sigma}_1)^{-1})$, and $\tau_2 (= -(\mathrm{Re}\hat{\sigma}_2)^{-1})$ are plotted for the pure O case with set 1 for rates of reactions (5) and (6) and the fast profile of a. The possibility of complex $\hat{\sigma}_1$ and $\hat{\sigma}_2$ merely means that the coupling results in an oscillating decay of the

perturbations. The time scale $\mathcal{B}^{-1}$ is several years at 22 km and decreases to about 90 minutes at 50 km and then increases above to about 1/10 day at 61 km. When coupling is included the actual time scale for thermal relaxation is τ_1 and for ozone relaxation is τ_2. As shown in Figure 7 coupling results in a slightly more rapid ozone relaxation below 30 km and a slightly slower ozone relaxation above 30 km.

Below 30 km coupling causes a slower thermal relaxation. If we write eqs (79) and (80) as

$$\hat{\sigma}_1 = -\frac{(a+\mathcal{B})}{2} - \delta/2 \tag{81}$$

$$\hat{\sigma}_2 = -\frac{(a+\mathcal{B})}{2} - \delta/2 \tag{82}$$

where $\delta \equiv [(a-\mathcal{B})^2 - 4\mathcal{J}\eta]^{1/2}$ and then substitute eqs (81) and (82) into eq (78), the result is

$$T' = \frac{T(0)}{2\delta} e^{-\frac{(a+\mathcal{B})}{2}t} [(\mathcal{B}-a)(e^{\delta/2t} - e^{-\delta/2t}) + \delta(e^{\delta/2t} + e^{-\delta/2t})]. \tag{83}$$

Now $\delta/2 < (\alpha + \beta)/2$ and if we consider an expansion of $e^{\pm\delta/2t}$ for time $< (\delta/2)^{-1}$ then we may write eq (83) as

$$T' \approx T(0)e^{-\frac{(\alpha+\beta)}{2}t}\left[1 - \frac{(\alpha-\beta)}{2}t\right] \tag{84}$$

or

$$T' \approx T(0)e^{-\alpha t}. \tag{85}$$

Thus, if we are considering a wave with period $\tau < \alpha^{-1}$, then the actual time scale for thermal relaxation is not τ_1 but α^{-1} below 30 km where eqs (84) and (85) are good approximations to eq (83).

Above 30 km β^{-1} is much less than α^{-1}, and coupling between the photochemical and radiative processes results in more rapid thermal relaxation as shown in Figure 7. Lindzen and Goody (1965) also found that thermal relaxation was more rapid above 30 km, though they used a different set of rates for reactions (5) and (6).

Above 40 km, $4(\gamma\eta + \alpha\beta) \ll (\alpha + \beta)^2$ and $\beta^{-1} \ll \alpha^{-1}$ so eq (81) can be approximated:

$$\hat{\sigma}_1 \approx -\frac{\gamma\eta}{\beta}. \tag{86}$$

For the pure O case eqs (68) and (70) reduce to

$$\beta = 2A\bar{\varphi} \tag{87}$$

$$\gamma = \alpha A\bar{\varphi}\frac{\bar{\varphi}}{\bar{T}}. \tag{88}$$

Use of eqs (87) and (88) in eq (86) yields

$$\hat{\sigma}_1 \approx -\frac{\alpha A \overline{r\omega}/\overline{T}}{2\overline{A\varphi}} = -\frac{\alpha \overline{r\omega}}{2\overline{T}}. \tag{89}$$

Substitution of eq (51) into eq (89) gives

$$\hat{\sigma}_1 \approx -\frac{\alpha a}{2}\left(1 - \frac{180^{\circ}}{\overline{T}}\right). \tag{90}$$

From Figures 2 and 4 we see that the equilibrium temperature for the pure O case is nearly constant above 40 km so, from eq (90)

$$\hat{\sigma}_1 \approx \text{constant above 40 km}$$

as is shown in Figure 7.

The N + H + O case requires the solution of eq (75). In Figure 8 are plotted the values α^{-1}, β^{-1}, and ε^{-1} as well as τ_1, τ_2, and $\tau_3 (= -[\mathrm{Re}\sigma_3]^{-1})$, where τ_3 is the hydroxyl relaxation time scale when coupling is included. Set 1 is used for rates for reactions (5) and (6) and the fast profile is used for α. The water vapor mixing ratio is $5 \cdot 10^{-6}$ while the low mixing ratio profile for the nitrogen oxides is used. In Figure 8 we see that below 40 km $\tau_3 \approx \varepsilon^{-1}$ and τ_1 and τ_2 are approximately the same as for the pure O case. This result is reasonable since

we previously found that inclusion of the hydrogen reactions has little effect on the equilibrium distribution of temperature and ozone density below 40 km. The only effect of the nitrogen reactions is to shorten $\mathcal{B}^{-1}$ at the lowest altitudes.

Above 40 km the hydrogen reactions become increasingly important with $\mathcal{E}^{-1}$ nearly the same size as $\mathcal{B}^{-1}$. The time scale for relaxation of a perturbation in the ozone density or hydroxyl density is modified since there is strong coupling between the ozone and hydrogen photochemistry. The photochemical acceleration of the thermal relaxation is modified but not eliminated. Above 40 km eq (86) is applicable and:

$$\sigma_1 \approx -\mathcal{J}\eta/\mathcal{B}. \tag{91}$$

For the N + H + O case above 40 km eqs (68) and (70) reduce to:

$$\mathcal{B} \approx B\psi_1 \tag{92}$$

$$\mathcal{J} \approx \beta B\overline{\psi\varphi}/\overline{T} \tag{93}$$

so substitution of eqs (92), (93), and (53) into eq (91) yields

$$\sigma_1 \approx \beta\eta\overline{\varphi}/\overline{T} = \beta\alpha\left(1 - \frac{180^{\circ}}{\overline{T}}\right). \tag{94}$$

Now the equilibrium temperature for the N - H - O case in Figures 2 and 4 decreases nearly linearly above 42 km and this decrease is reflected in the nearly linear increase of τ_1 with height in Figure 8.

Figure 9 shows τ_1 for six cases: O, H + O, N + O (low), N + O (high), N + H + O (low), and N + H + O (high). It is apparent that inclusion of nitrogen reactions for the low mixing ratio of nitrogen oxides does not alter τ_1 from cases with no nitrogen present but use of the high mixing ratio increases τ_1. The reason for this effect can be seen most readily by referring to the equilibrium eqs (49), (50), and (51). The effect of nitrogen reactions on ozone density is contained in the term $-F\varphi X$ and above 35 km this term can be written, by application of eqs (29), (14), and (9), as:

$$F\varphi X \approx 2k_{17}K\varphi n_m \tag{95}$$

The effect of the pure oxygen reactions on ozone density is contained in the term, $-A\varphi^2$ and from eqs (26) and (9), we have

$$A\varphi^2 = \frac{2(q_{3a} + q_{3b})}{n_{O_2}} (k_6/k_5)\varphi^2. \tag{96}$$

Comparing the terms (95) and (96), we see that temperature dependence of ozone density due to nitrogen reactions is by k_{17} and the temperature dependence of ozone density due the oxygen reactions is by $(k_6/k_5)^{1/2}$. The temperature dependence of k_{17} is much less than that of $(k_6/k_5)^{1/2}$. When the high mixing ratio profile of nitrogen oxides is used, $F\varphi X$

becomes more important than $A\varphi^2$ in determining the ozone density between 35 and 45 km. Since the temperature dependence of $F\varphi X$ is less than that of $A\varphi^2$, it follows that τ_1 is increased at heights where nitrogen reactions are more important than pure O reactions in determining ozone density.

Figure 10 shows τ_1 for the N + H + O (low) case when three different sets of rates for reactions (5) and (6) and two values for α, fast and slow are used. Above 35 km eq (94) still holds,

$$\sigma_1 \approx \beta \alpha (1 - \frac{180^\circ}{\bar{T}}). \qquad (97)$$

Since the equilibrium temperature varies with different sets of rates for reactions (5) and (6) (Figure 7), so does σ_1.

As discussed in section 4, the effect of varying rates for reactions (7)-(18) can be shown by varying the water vapor mixing ratio or the mixing ratio of nitrogen oxides. Resulting values of τ_1 are within the range of those shown in Figures 9 and 10.

In section 4 we found that the equilibrium temperature calculated had the best match with the observed temperature for the case with set 1 for the rates for reactions (5) and (6), the cooling time scale of α^{-1} = 10 days, a water vapor mixing ratio of $5 \cdot 10^{-7}$, and a nitrogen oxides mixing ratio defined by Profile 7. Using these parameters in the present calculations we find that the minimum value of τ_1 is

2.6 days at 32 km. Between 35 and 61 km the value of τ_1 is between 3.3 and 3.7 days. Since σ_1 is proportional to 'a', the revisions suggested in section 4a will lead to further reductions of τ_1.

The results show that coupling between radiative and photochemical processes leads to an acceleration of thermal relaxation above 30 km for a wide range of reaction rates and other parameters. The minimum value of τ_1 is between 2 and 4 days at 31-35 km. When the hydrogen reactions are neglected τ_1 is nearly constant with height above 40 km and when the hydrogen reactions are included with a mixing ratio of $5 \cdot 10^{-6}$ for water vapor τ_1 increases almost linearly from the minimum value at 35 km to about 5 days at 61 km. Therefore the Newtonian cooling rate coefficient to be used in the temperature equation for dynamical problems in the stratosphere above 30 km is not 'a' but τ_1^{-1}. Moreover τ_1^{-1} seems large enough to dissipate internal Rossby waves.

6. CONCLUSIONS

In this paper we have developed quantitatively justifiable simple models for the radiative heating and the complicated ozone photochemistry of the stratosphere between about 20 and 60 km. These models permit the immediate evaluation of the effects of various chemical and physical quantities on the temperature and ozone distributions in the stratosphere. We show that the region 35-60 km should (away from arctic regions) be in approximately joint radiative-photochemical equilibrium, and we use our simple models to calculate this equilibrium. We show that the interaction of radiation and chemistry significantly buffers the temperature and ozone distributions in the stratosphere so that rather large changes in cooling rates, reaction rates, etc., lead to much more modest changes in ozone and temperature. We also show that given an observed distribution of mean temperature (a quantity much more extensively measured than ozone) we can (assuming accurate knowledge of reaction and infrared cooling rate coefficients) determine the amounts of water vapor and nitrogen oxides needed to produce the ozone distribution which would in turn lead to the observed temperature. This procedure is facilitated by the fact (which we demonstrate) that hydrogen reactions are significant loss processes for ozone above 40 km while nitrogen reactions are important below 50 km. Thus there are regions where nitrogen and hydrogen reactions are individually rather than jointly important. Unfortunately, reaction and cooling rate coefficients are not accurately known. However, our simplified equations can still be used as diagnostic tools. In this manner, we show that an

internally consistent description of observed distributions of temperature and ozone in the stratosphere can be obtained with a time scale for infrared cooling varying from ten days at 35 km to 7.7 days above 40 km, a mixing ratio for nitrogen oxides ($NO + NO_2$) of about $2\text{-}3 \cdot 10^{-8}$ and a mixing ratio for water of about $3 \cdot 10^{-6}$. The question of normal NO_x mixing ratio has assumed considerable importance recently because it is believed that proposed SST (super sonic transport) operations may add about $1 \cdot 10^{-9}$ to the NO_x mixing ratio. The present calculations suggest that the SST contribution will be only 3-5% of the ambient amount, and because of the thermal buffering of the system the effect of this addition on ozone density should be less than 3-5%.

We also used our simple models to calculate the joint radiative-photochemical relaxation of perturbations in temperature, ozone mixing ratio and hydroxyl mixing ratio away from their equilibrium values. We find that for all photochemical models considered, the photochemistry greatly accelerates thermal relaxation as calculated simply on the basis of infrared cooling. The time scale for the latter is about 10 days. The actual time scale for thermal relaxation when photochemistry (which is temperature dependent) is included proves to be only 2-4 days. These shorter scales imply greatly enhanced damping for hydrodynamic waves in the stratosphere.

ACKNOWLEDGMENTS

The bulk of this work has been supported by grant number GA-25904 of the National Science Foundation and grant number NGR 14-001-193 of the National Aeronautics and Space Administration, both at the University of Chicago. Additional support was received under grant number NSF GA 33990X of the National Science Foundation at Harvard University. Computations were performed at the National Center for Atmospheric Research which is supported by the National Science Foundation. Useful conversations with S. Wofsy are also gratefully acknowledged.

REFERENCES

Barth, Charles A., "Nitric Oxide in the Upper Atmosphere," Annales de Geophysique, Vol. 22, No. 2, Lille, France, April-June 1966, pp. 198-207.

Benson, Sidney W., and Axworthy, Arthur E., "Reconsideration of the Rate Constants From the Thermal Decomposition of Ozone," Journal of Chemical Physics, Vol. 42, No. 7, 1 April 1965, pp. 2614-2615.

Berces, T. and Förgeteg, S., "Kinetics of Photolysis of Nitric Acid Vapour, Part 2, Decomposition of Nitric Acid Vapour Photosensitized by Nitrogen Dioxide," Transactions of the Faraday Society, Vol. 66, No. 567, Part 3, London, England, March 1970, pp. 640-647.

Brinkmann, R. T., "Dissociation of Water Vapor and Evolution of Oxygen in the Terrestrial Atmosphere," Journal of Geophysical Research, Vol. 74, No. 23, 20 October 1969, pp. 5355-5368.

Brinkmann, R. T., Green, A. E. S., and Barth, Charles A., "A Digitalized Solar Ultraviolet Spectrum," Technical Report No. 32-951, Jet Propulsion Laboratory, California Institute of Technology, Pasadena, California, 15 August 1966, 73 pp.

Charney, Jule G., and Drazin, Philip G., "Propagation of Planetary-Scale Disturbances From the Lower into the Upper Atmosphere," Journal of Geophysical Research, Vol. 66, No. 1, January 1961, pp. 83-109.

Crutzen, Paul J., "Ozone Production Rates in an Oxygen-Hydrogen-Nitrogen Oxide Atmosphere," Journal of Geophysical Research, Oceans and Atmospheres, Vol. 76, No. 30, 20 October 1971, pp. 7311-7327.

Demore, W. B., and Raper, O. F., "Reaction of O('D) With Methane," Journal of Chemical Physics, Vol. 46, No. 7, 1 April 1967, pp. 2500-2505.

Dickinson, Robert E., "On the Excitation and Propagation of Zonal Winds in an Atmosphere With Newtonian Cooling," Journal of the Atmospheric Sciences, Vol. 25, No. 2, March 1968, pp. 269-279.

Dickinson, Robert E., "Vertical Propagation of Planetary Rossby Waves Through an Atmosphere With Newtonian Cooling," Journal of Geophysical Research, Vol. 74, No. 4, 15 February 1969, pp. 929-938.

Donovan, R. J., and Husain, D., "Recent Advances in the Chemistry of Electronically Excited Atoms," Chemical Reviews, Vol. 70, No. 4, August 1970, pp. 489-516.

Dütsch, H. U., "The Photochemistry of Stratospheric Ozone," Quarterly Journal of the Royal Meteorological Society, Vol. 94, No. 402, London, England, October 1968, pp. 483-497.

Greiner, N. R., "Hydroxal Radical Kinetics by Kinetic Spectroscopy, III; Reactions With H_2O_2 in the Range 300°-458°K," Journal of Physical Chemistry, Vol. 72, No. 2, February 1968, pp. 857-859.

Griggs, M., "Absorption Coefficients of Ozone in the Ultraviolet and Visible Regions," Journal of Chemical Physics, Vol. 49, No. 2, 15 July 1968, pp. 857-859.

Hall, Jr., T. C., and Blacet, F. E., "Separation of the Absorption Spectra of NO_2 and N_2O_4 in the Range 2400-5000 Å," Journal of Chemical Physics, Vol. 20, No. 11, November 1952, pp. 1745-1749.

Hilsenrath, Ernest, Seiden, Lester, and Goodman, Philip, "An Ozone Measurement in the Mesosphere and Stratosphere by Means of a Rocket Sonde," Journal of Geophysical Research, Oceans and Atmospheres, Vol. 74, No. 28, 20 December 1969, pp. 6873-6880.

Hinteregger, H. E., "The Extreme Ultraviolet Solar Spectrum and its Variation During a Solar Cycle," Annales de Geophysique, Vol. 26, No. 2, Lille, France, April-June 1970, pp. 547-554.

Holt, R. B., McLane, C. K., and Oldenberg, O., "Ultraviolet Absorption Spectrum of Hydrogen Peroxide," Journal of Chemical Physics, Vol. 16, No. 3, March 1948, pp. 225-229.

Holton, James R., "A Diagnostic Model for Equatorial Wave Disturbances: The Role of Vertical Shear of the Mean Wind," Journal of the Atmospheric Sciences, Vol. 28, No. 1, January 1971, pp. 55-64.

Hudson, R. D., Carter, V. L., and Breig, E. J., "Predissociation in the Schumann-Runge Band System of O_2: Laboratory Measurements and Atmospheric Effects," Journal of Geophysical Research, Space

Physics, Vol. 74, No. 16, 1 August 1969, pp. 4079-4087.

Hunt, B. G., "Photochemistry of Ozone in a Moist Atmosphere," Journal of Geophysical Research, Vol. 71, No. 5, 1 March 1966, pp. 1385-1398.

Inn, Edward C. Y., and Tanaka, Yoshio, "Absorption Coefficient of Ozone in the Ultraviolet and Visible Regions," Journal of the Optical Society of America, Vol. 43, No. 10, October 1953, pp. 870-873.

Jefferys, Sir Harold, "The Instability of a Compressible Fluid Heated Below," Proceedings of the Cambridge Philosophical Society, Vol. 26, Part 2, London, England, April 1930, pp. 170-172.

Johnson, Francis S., Purcell, James D., and Tousey, Richard, "Studies of the Ozone Layer Above New Mexico," Rocket Exploration of the Upper Atmosphere, ed. R. L. S. Boyd and M. J. Seaton, Pergamon Press, London, England, 1954, pp. 189-199.

Johnston, Harold, "Laboratory Chemical Kinetics as an Atmospheric Science", Proceedings of the Survey Conference, February 15-16, 1972, Climatic Impact Assessment Program, A. E. Barrington, editor. Department of Transportation report DOT-TSC-OST-72-13. Available through National Technical Information Service, Springfield, Virginia 22151, pp. 90-114.

Johnston, Harold S., and Yost, Don M., "The Kinetics of the Rapid Gas Reaction Between Ozone and Nitrogen Dioxide," Journal of Chemical Physics, Vol. 17, No. 4, April 1949, pp. 386-392.

Junge, C. E., "Gases," Air Chemistry and Radioactivity, ed. J. Van Mieghem, Vol. 4, Academic Press, New York, 1963, Chapter 1, p. 37.

Kaufman, Fredrick, "Neutral Reactions," DASA Reaction Rate Handbook, 1967, Chapter 14, pp. 1-17.

Kaufman, Fredrick, "Neutral Reactions Involving Hydrogen and Other Minor Constituents," Canadian Journal of Chemistry, Vol. 47, No. 10, Ottawa, Canada, 15 May 1969, pp. 1917-1926.

Klein, Fritz S., and Herron, John T., "Erratum: Mass-Spectrometric Study of the Reactions of O Atoms with NO and NO_2," Journal of Chemical Physics, Vol. 44, No. 9, 1 May 1966, pp. 3645-3646.

Kondratyev, K. Ya., Radiation in The Atmosphere, International Geophysics Series, Vol. 12, Academic Press, New York 1969, 912 pp.

Leovy, Conway, "Radiative Equilibrium of the Mesosphere", Journal of the Atmospheric Sciences, Vol. 21, No. 3, May 1964a, pp. 238-248.

Leovy, Conway, "Simple Models of Thermally Driven Mesospheric Circulation", Journal of the Atmospheric Sciences, Vol. 21, No. 4, July 1964b, pp. 327-341.

Leovy, Conway B., "Atmospheric Ozone: An Analytic Model for Photochemistry in the Presence of Water Vapor," Journal of Geophysical Research, Vol. 74, No. 2, 15 January 1969a, pp. 417-426.

Leovy, Conway B., "Energetics of the Middle Atmosphere," Advances in Geophysics, Vol. 13, Academic Press, New York, 1969b, pp. 191-221.

Lindzen, Richard S. and Blake, Donna, "Internal Gravity Waves in Atmospheres with Realistic Dissipation and Temperature Part II. Thermal Tides Excited Below the Mesopause", Geophysical Fluid Dynamics, Vol. 2, No. 1, 1971, pp. 31-61.

Lindzen, Richard S. and Goody, Richard, "Radiative and Photochemical Processes in Mesospheric Dynamics: Part I, Models for Radiative and Photochemical Processes," Journal of the Atmospheric Sciences, Vol. 22, No. 4, July 1965, pp. 341-348.

Mastenbrook, H. J., "Water Vapor Distribution in the Stratosphere and High Troposphere," Journal of the Atmospheric Sciences, Vol. 25, No. 2, March 1968, pp. 299-311.

Miller, D. E., and Stewart, K. H., "Observations of Atmospheric Ozone," Proceedings of the Royal Society of London, Series A, Vol. 288, No. 1415, England, 30 November 1965, pp. 540-544.

Murgatroyd, R. J., and Goody, Richard M., "Sources and Sinks of Radiative Energy From 30 to 90 km," Quarterly Journal of the Royal Meteorological Society, London, England, Vol. 84, No. 361, July 1958, pp. 205-234.

Nakayama, Toshio, Kitamura, Morris Y., and Watanabe, K., "Ionization Potential and Absorption Coefficients of Nitrogen Dioxide," Journal of Chemical Physics, Vol. 30, No. 5, May 1959, pp. 1180-1186.

Nicolet, M., "Ozone and Hydrogen Reactions," Annales de Geophysique, Vol. 26, No. 2, Lille, France, April-June 1970, pp. 547-554.

Ogura, Yoshimitsu, and Phillips, Norman A., "Scale Analysis in Deep and Shallow Convection in the Atmosphere," Journal of the Atmospheric Sciences, Vol. 19, No. 2, March 1962, pp. 173-179.

Pearce, Jeffery B., "Rocket Measurement of Nitric Oxide Between 60 and 96 km," Journal of Geophysical Research, Space Physics, Vol. 74, No. 3, 1 March 1969, pp. 853-861.

Phillips, L. F. and Schiff, H. I., "Mass Spectrometric Studies of Atomic Reactions. III Reactions of Hydrogen with Nitrogen Dioxide and with Ozone", Journal of Chemical Physics, Vol. 37, No. 6, September 1962, pp. 1233-1238.

Plass, Gilbert N., "The Influence of the 9.6 Micron Ozone Band on the Atmospheric Infra-Red Cooling Rate," Quarterly Journal of the Royal Meteorological Society, London, England, Vol. 82, No. 351, January 1956, pp. 30-44.

Rawcliffe, R. D., Meloy, G. E., Friedman, R. M., and Rodgers E. H., "Measurement of Vertical Distribution of Ozone From a Polar Orbiting Satellite," Journal of Geophysical Research, Vol. 68, No. 24, 15 December 1963, pp. 6425-6429.

Rodgers, C. D., and Walshaw, C. D., "The Computation of Infrared Cooling in Planetary Atmospheres," Quarterly Journal of the Royal Meteorological Society, London, England, Vol. 92, No. 392, January 1966, pp. 67-92.

Schiff, H. I., "Neutral Reactions Involving Oxygen and Nitrogen," Canadian Journal of Chemistry, Vol. 47, No. 10, Ottawa, Canada, 15 May 1969, pp. 1903-1916.

Schofield, K., "An Evaluation of Kinetic Rate Data for Reactions of Neutrals of Atmospheric Interest," Planetary and Space Sciences, Vol. 15, No. 4, Oxford, England, April 1967, pp. 643-670.

Schölz, T. G., Ehhalt, D. H., Heidt, L. E., and Martell, E. A., "Water Vapor, Molecular Hydrogen, Methane, and Tritium Concentrations Near the Stratopause," Journal of Geophysical Research, Vol. 75, No. 15, 20 May 1970, pp. 3049-3054.

Schütz, K., Junge, C., Beck, R., and Albrecht, B., "Studies of Atmospheric N_2O," Journal of Geophysical Research, Vol. 75, No. 12, 20 April 1970, pp. 2230-2246.

Shimazaki, Tatsuo, and Laird, A. R., "A Model Calculation of the Diurnal Variation in Minor Neutral Constituents in the Mesosphere

and Lower Thermosphere Including Transport Effects," Journal of Geophysical Research, Space Physics, Vol. 75, No. 16, 1 June 1970, pp. 3221-3235.

Supplementary Atmosphere (Tropical), Handbook of Geophysics and Space Environments, ed. Shea L. Valley, Air Force Cambridge Research Laboratories, McGraw-Hill, New York, 1965, pp. 2-11.

Theon, J. S., and Smith, W. S., "The Meteorological Structure of the Mesosphere Including Seasonal and Latitudinal Variations," Mesospheric Models and Related Experiments, Proceedings of the Fourth Esrin-Eslab Symposium, Frascati, Italy, 6-10 July 1970, ed. G. Fiocco, Astrophysics and Space Science Library, Vol. 25, D. Reidel Publishing Company, Dordrecht, Holland, 1971, pp. 131-146.

Thompson, B. A., Harteck, P., and Reeves, Jr., R. R., "Ultraviolet Absorption Coefficients of CO_2, CO, O_2, H_2O, N_2O, NH_3, NO, SO_2, and CH_4 Between 1850 and 4000 Å," Journal of Geophysical Research, Vol. 68, No. 24, 15 December 1963, pp. 6431-6436.

Van Allen, J. A. and Hopfield, J. J., "Preliminary Report on Atmospheric Ozone Measurements from Rockets", Societé Royale des Sciences de Liege - Memoires, Vol. 12, Belgium, 1952, pp. 179-183.

Watanabe, K., and Zelikoff, Murray, "Absorption Coefficients of Water Vapor in the Vacuum Ultraviolet," Journal of the Optical Society of America, Vol. 43, No. 9, September 1953, pp. 753-755.

Weeks, L. H., and Smith, L. G., "A Rocket Measurement of Ozone Near Sunrise," Planetary and Space Science, Vol. 16, No. 9. Oxford, England, September 1968, pp. 1189-1195.

Wofsy, Steven C., McConnell, John C., and McElroy, Michael B., "Atmospheric CH_4, CO, and CO_2", Journal of Geophysical Research. Vol. 77, No. 24, August 1972, pp. 4477-4493.

Zipf, E. C., "The Collisional Deactivation of Metastable Atoms and Molecules in the Upper Atmosphere," Canadian Journal of Chemistry, Vol. 47, No. 10, Ottawa, Canada, 15 May 1969, pp. 1863-1877.

Table 1

	Reaction	Rate	Source
1.	$O_2 + h\nu \rightarrow O + O$	$q_2(\lambda < 2460$ Å)	See text
2a.	$O_3 + h\nu \rightarrow O + O_2$	$q_{3a}(3100$ Å $< \lambda < 11000$ Å)	See text
2b.	$O_3 + h\nu \rightarrow O^* + O_2$	$q_{3b}(\lambda < 3100$ Å)	See text
3.	$H_2O + h\nu \rightarrow H + OH$	$q_{H_2O}(\lambda < 2400$ Å)	See text
4.	$NO_2 + h\nu \rightarrow NO + O$	$q_{NO_2}(\lambda < 3975$ Å)	See text
5.	$O + O_2 + M \rightarrow O_3 + M$	k_5 see Table 2	See Table 2
6.	$O + O_3 \rightarrow 2O_2$	k_6 see Table 2	See Table 2
7.	$O^* + M \rightarrow O + M$	$k_7 = 5 \cdot 10^{-11}$	Zipf 1969
8.	$O^* + H_2O \rightarrow 2OH$	$k_8 = 5 \cdot 10^{-11}$	Demore and Raper 1967
9.	$OH + O \rightarrow H + O_2$	$k_9 = 5 \cdot 10^{-11}$	Kaufman 1969
10.	$H + O_2 + M \rightarrow HO_2 + M$	$k_{10} = 4 \cdot 10^{-32}$	Kaufman 1969
11.	$HO_2 + O \rightarrow OH + O_2$	$k_{11} = 5 \cdot 10^{-11}$	Nicolet 1970
12.	$OH + O_3 \rightarrow HO_2 + O_2$	k_{12} 1.7·10^{-12}T$^{1/2}$exp(-1500/T)	Nicolet 1970
13.	$OH + OH \rightarrow H_2O + O$	$k_{13} = 5 \cdot 10^{-13} T^{1/2} \exp(-1000/T)$	Nicolet 1970

Table 1 (Cont'd.)

	Reaction	Rate	Source
14.	$OH + HO_2 \rightarrow H_2O + O_2$	$k_{14} = 10^{-11}$	Kaufman 1969
15.	$HO_2 + NO \rightarrow OH + NO_2$	$k_{15} = 3 \cdot 10^{-12} T^{1/2} \exp(-1250/T)$	Nicolet 1970
16.	$NO_2 + O \rightarrow NO + O_2$	$k_{16} = 3.2 \cdot 10^{-11} \exp(-300/T)$	Klein and Herron 1966
17.	$NO + O_3 \rightarrow NO_2 + O_2$	$k_{17} = 1.7 \cdot 10^{-12} \exp(-1310/T)$	Schofield 1967
18.	$NO_2 + O_3 \rightarrow NO_3 + O_2$	$k_{18} = 10^{-11} \exp(-3500/T)$	Johnston and Yost 1949
19.	$NO_2 + OH + M \rightarrow HNO_3 + M$	$k_{19} = 3.3 \cdot 10^{-33}$	Berces and Förgeteg 1970
20.	$NO + OH + M \rightarrow HNO_2 + M$	$k_{20} = k_{19}$	See text
21.	$HNO_3 + O \rightarrow NO_3 + OH$	$k_{21} = 1.7 \cdot 10^{-11}$	Berces and Förgeteg 1970
22.	$HNO_2 + O \rightarrow OH + NO_2$	$k_{22} = k_{21}$	See text
23.	$NO_3 + NO \rightarrow 2NO_2$	$k_{23} = 10^{-11}$	Berces and Förgeteg 1970
24.	$HO_2 + HO_2 \rightarrow H_2O_2 + O_2$	$k_{24} = 5.10^{-12} \exp(-1000/T)$	Nicolet 1970
25.	$H_2O_2 + h\nu \rightarrow 2OH$	$\lambda < 5650$ Å	Holt 1948
26.	$H_2O_2 + OH \rightarrow H_2O + HO_2$	$k_{26} = 4.10^{-13} T^{1/2} \exp(-600/T)$	Greiner 1968
27.	$H + O_3 \rightarrow OH + O_2$	$k_{27} = 1.5 \cdot 10^{-12} T^{1/2}$	Phillips and Schiff 1962

Table 2

Set 1:	
$k_5 = 1.2 \cdot 10^{-35} \exp(1000/T)$ $k_6 = 2.0 \cdot 10^{-11} \exp(-2395/T)$	Schiff 1969
Set 2:	
$k_5 = 8.0 \cdot 10^{-35} \exp(445/T)$ $k_6 = 5.6 \cdot 10^{-11} \exp(-2850/T)$	Benson and Axworthy 1965
Set 3:	
$k_5 = 5.5 \cdot 10^{-34} (300/T)^{2.6}$ $k_6 = 1.4 \cdot 10^{-12} \exp(-1500/T)$	Kaufman 1967

Table 3

Nitrogen Oxides Profile	1	2	3	4	5	6	7	8
Nitrogen Oxides Mixing Ratio at Stratopause	$6.4 \cdot 10^{-9}$	$8.8 \cdot 10^{-8}$	$3 \cdot 10^{-9}$	$3 \cdot 10^{-8}$	10^{-7}	$1.4 \cdot 10^{-8}$	$1.6 \cdot 10^{-7}$	0
Temperature at Stratopause (^{o}K)	304	291	306	301	291	303	288	307
Temperature at Stratopause (Daily Mean)(^{o}K)							273	290

Figure Legends

Figure 1. The absorption of solar photons by NO_2, O_2, H_2O, and O_3 as a function of height.

Figure 2. The radiative-photochemical equilibrium temperature at 0° latitude as a function of height. The six cases are described in section 4.

Figure 3. The radiative-photochemical equilibrium ozone number density at 0° latitude as a function of height.

Figure 4. Same as Figure 2 but at 45° latitude.

Figure 5. Same as Figure 3 but at 45° latitude.

Figure 6. The radiative-photochemical equilibrium temperature as a function of height for 0° latitude for an N + H + O atmosphere. The three sets of reaction rates are in Table 2 and the fast and slow cooling rates are discussed in the text. Our low NO_x values were used.

Figure 7. The relaxation time scales in a pure O atmosphere. β^{-1} and a^{-1} are the relaxation time scales for O_3 and temperature, respectively, when the coupling between the photochemistry and temperature is neglected. τ_2 and τ_1 are the relaxation time scales for the O_3 and temperature, respectively, when the coupling is considered.

Figure 8. The relaxation time scales in an N + H + O atmosphere. $\mathcal{B}^{-1}$, $\mathcal{E}^{-1}$, and a^{-1} are the relaxation time scales for O_3, OH, and temperature, respectively, when the coupling between the photochemistry and temperature is neglected. τ_2, τ_3, and τ_1 are the relaxation time scales for O_3, OH, and temperature, respectively, when the coupling is included.

Figure 9. The thermal relaxation time scale, τ_1, as a function of height for the cases considered in Figures 2 and 3.

Figure 10. The thermal relaxation time scale, τ_1, as a function of height for the cases considered in Figure 6.

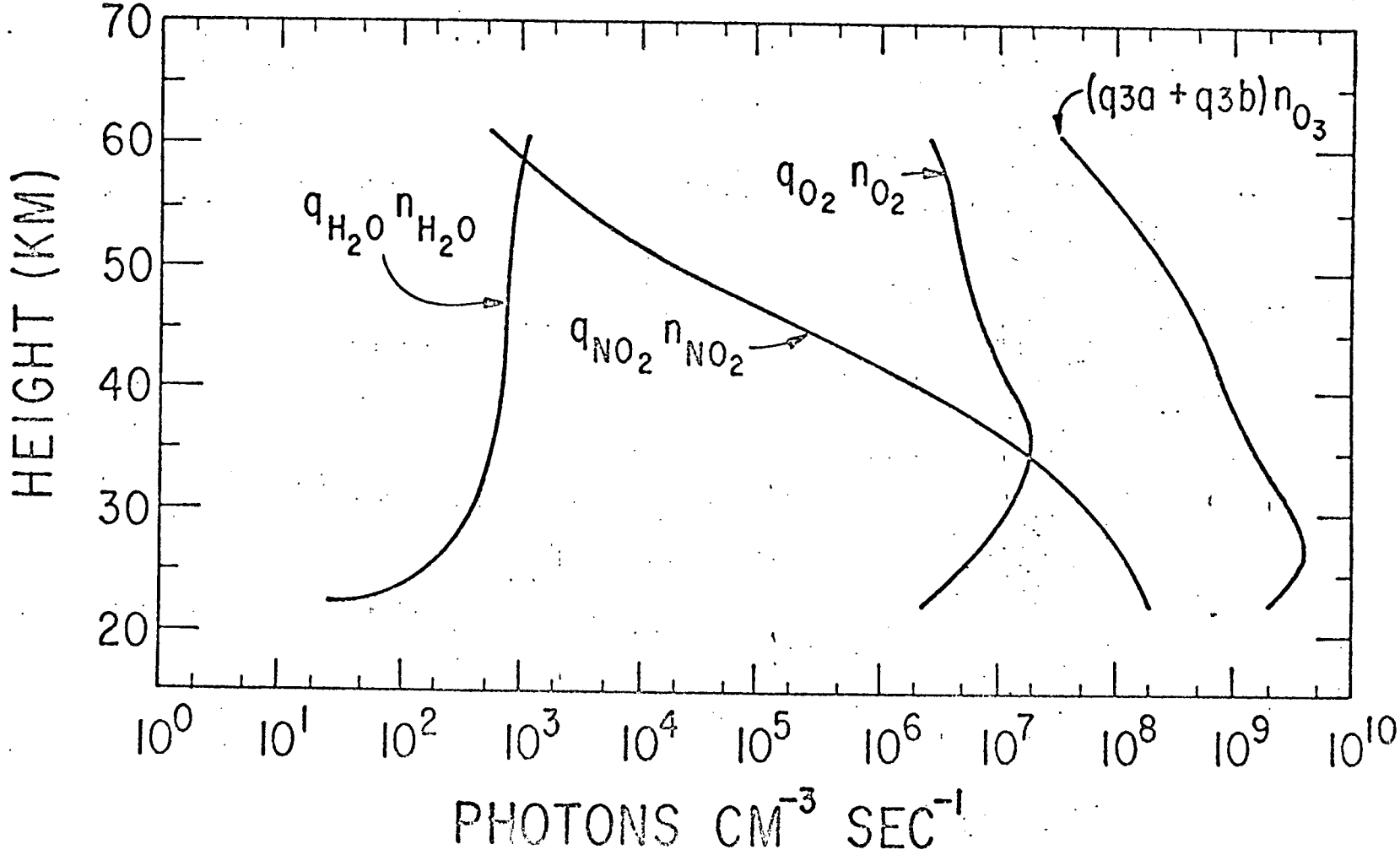
70
60
50
40
30
20
HEIGHT (KM)
$q_{H_2O}\, n_{H_2O}$
$q_{NO_2}\, n_{NO_2}$
$q_{O_2}\, n_{O_2}$
$(q_{3a} + q_{3b})\, n_{O_3}$
10^0 10^1 10^2 10^3 10^4 10^5 10^6 10^7 10^8 10^9 10^{10}
PHOTONS CM^{-3} SEC^{-1}

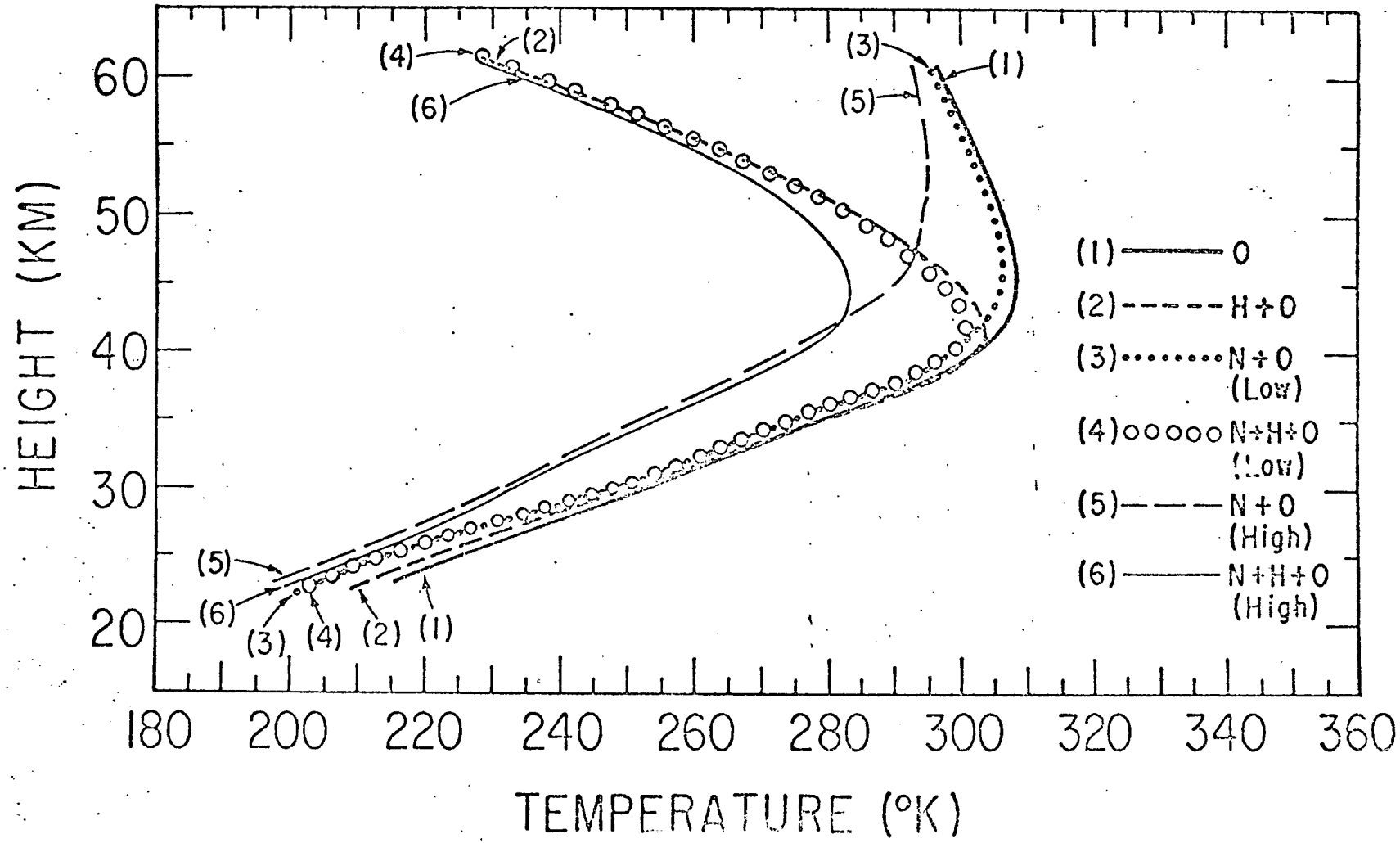
HEIGHT (KM)
60
50
40
30
20
180
200
220
240
260
280
300
320
340
360
TEMPERATURE (°K)
(1) O
(2) H+O
(3) N+O (Low)
(4) N+H+O (Low)
(5) N+O (High)
(6) N+H+O (High)
(4)
(2)
(3)
(1)
(5)
(6)
(5)
(6)
(3)
(4)
(2)
(1)

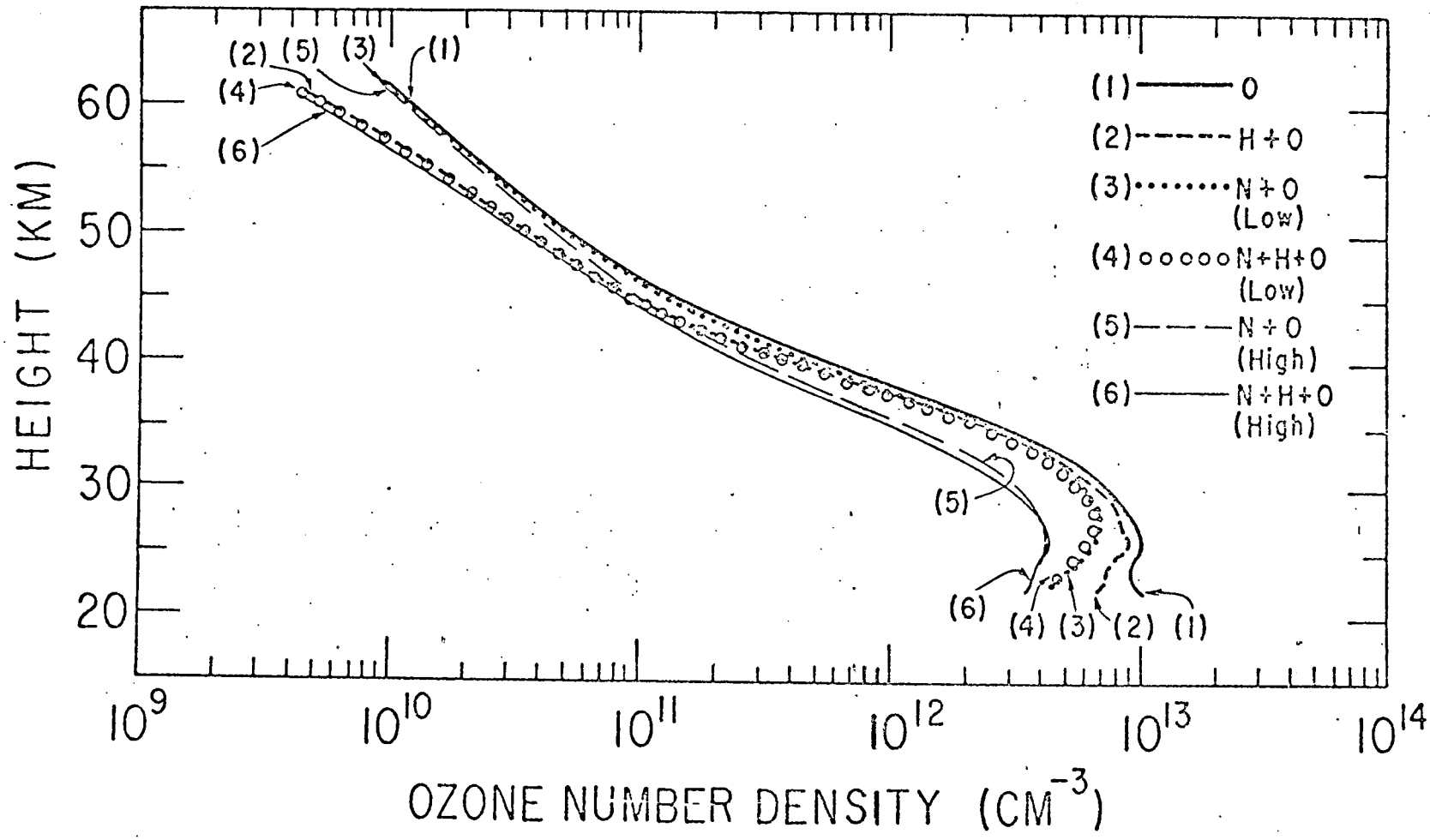
HEIGHT (KM)
60
50
40
30
20
10^9
10^{10}
10^{11}
10^{12}
10^{13}
10^{14}
OZONE NUMBER DENSITY (CM^{-3})
(1) O
(2) H + O
(3) N + O (Low)
(4) N + H + O (Low)
(5) N + O (High)
(6) N + H + O (High)

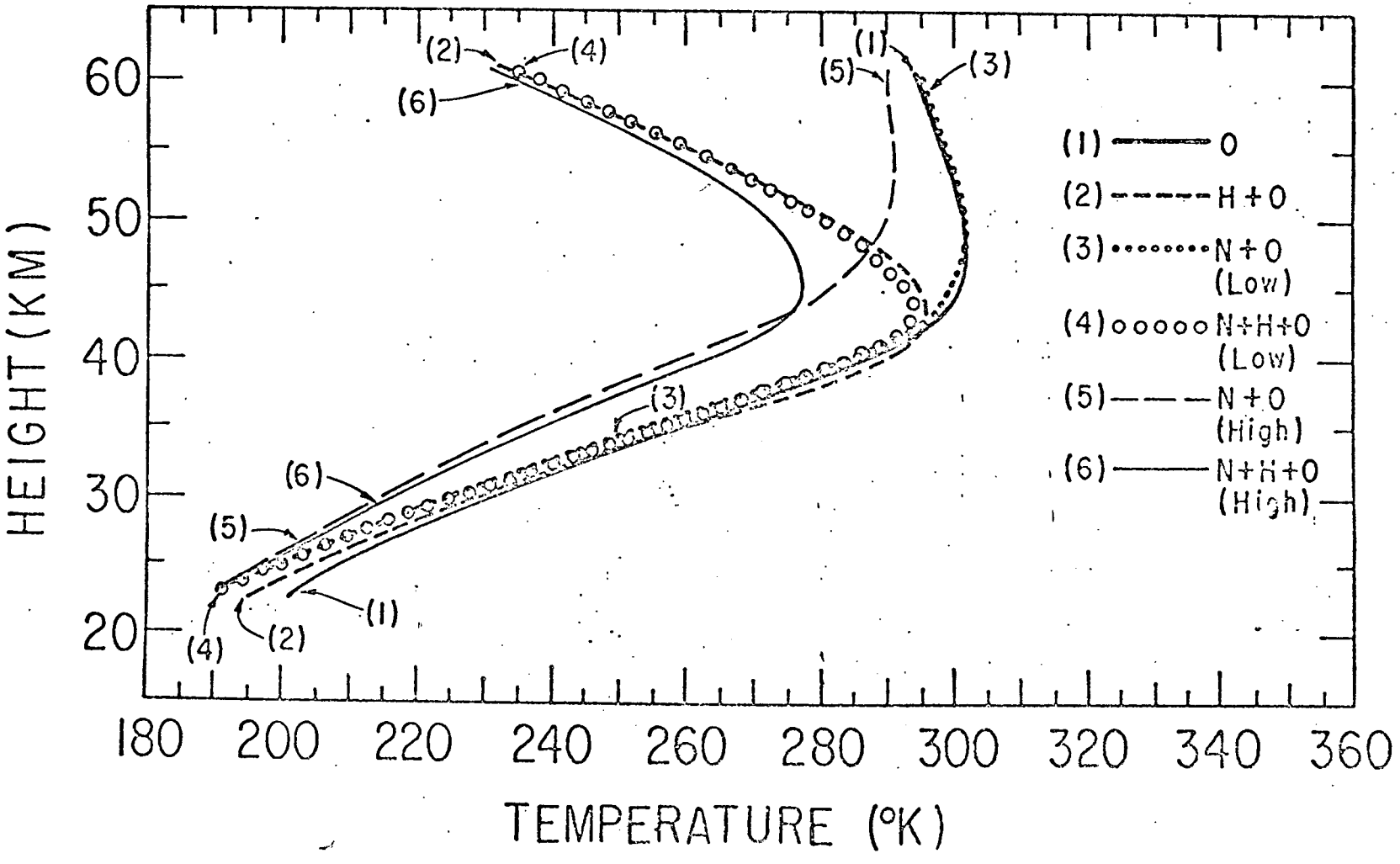
HEIGHT (KM)
60
50
40
30
20
180
200
220
240
260
280
300
320
340
360
TEMPERATURE (°K)
(1) O
(2) H+O
(3) N+O (Low)
(4) N+H+O (Low)
(5) N+O (High)
(6) N+H+O (High)

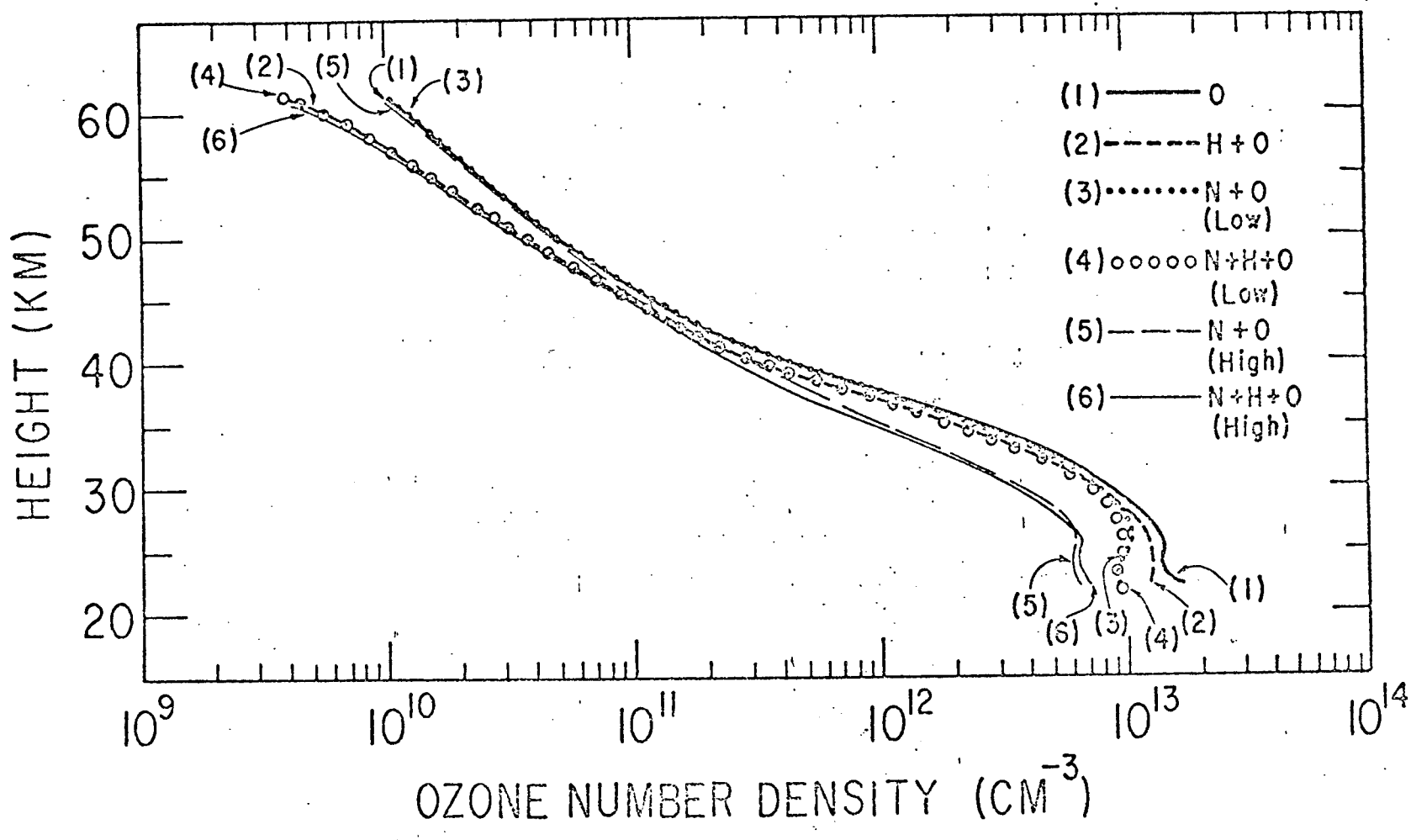
HEIGHT (KM)
60
50
40
30
20
10^9
10^{10}
10^{11}
10^{12}
10^{13}
10^{14}
OZONE NUMBER DENSITY (CM^{-3})
(1) —— O
(2) - - - - H + O
(3) ····· N + O (Low)
(4) ooooo N + H + O (Low)
(5) — — — N + O (High)
(6) —— N + H + O (High)
(4) (2) (5) (1) (3)
(6)
(5) (6) (3) (4) (2) (1)

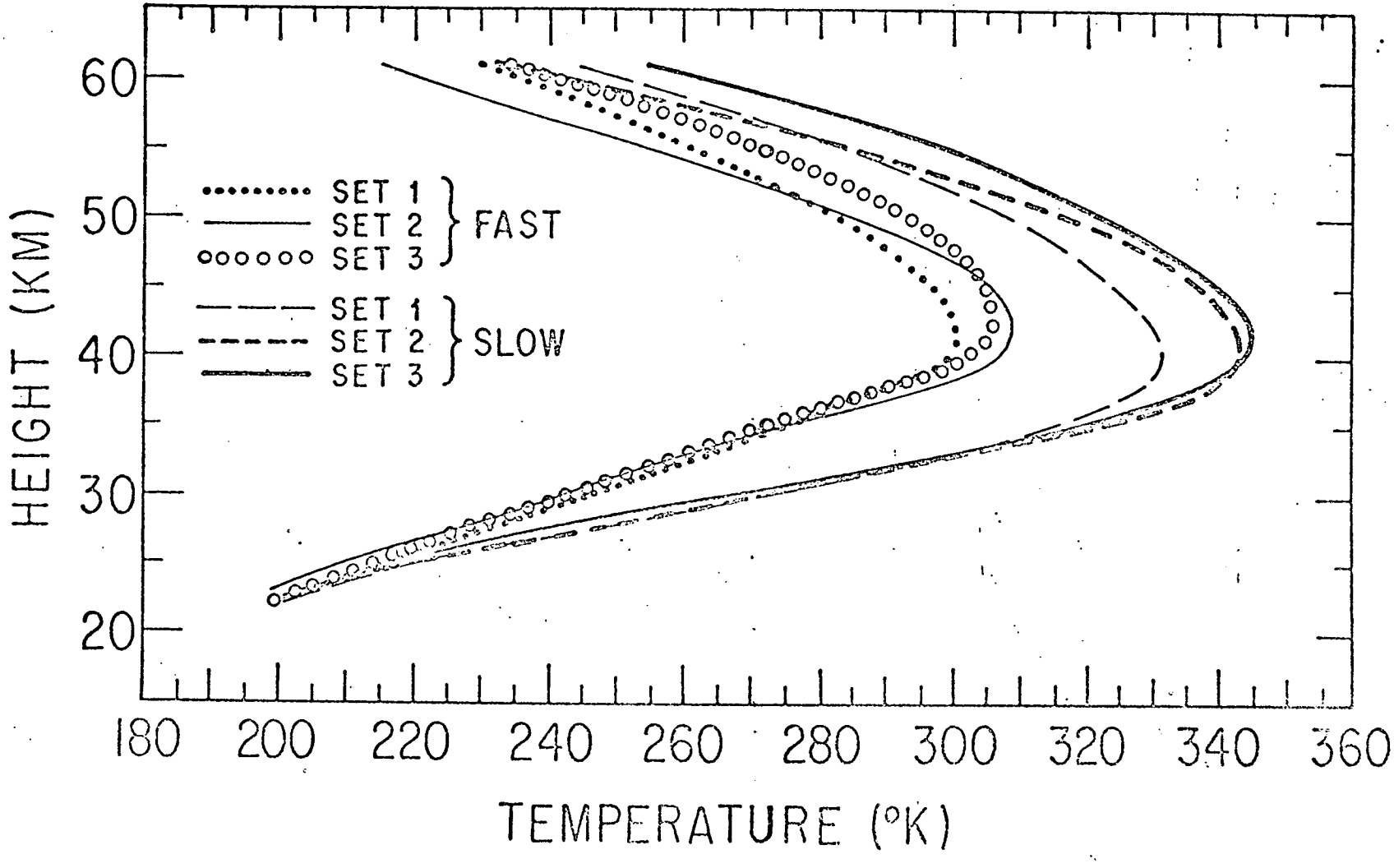
HEIGHT (KM)
60
50
40
30
20
SET 1
SET 2
SET 3
FAST
SET 1
SET 2
SET 3
SLOW
180
200
220
240
260
280
300
320
340
360
TEMPERATURE (°K)

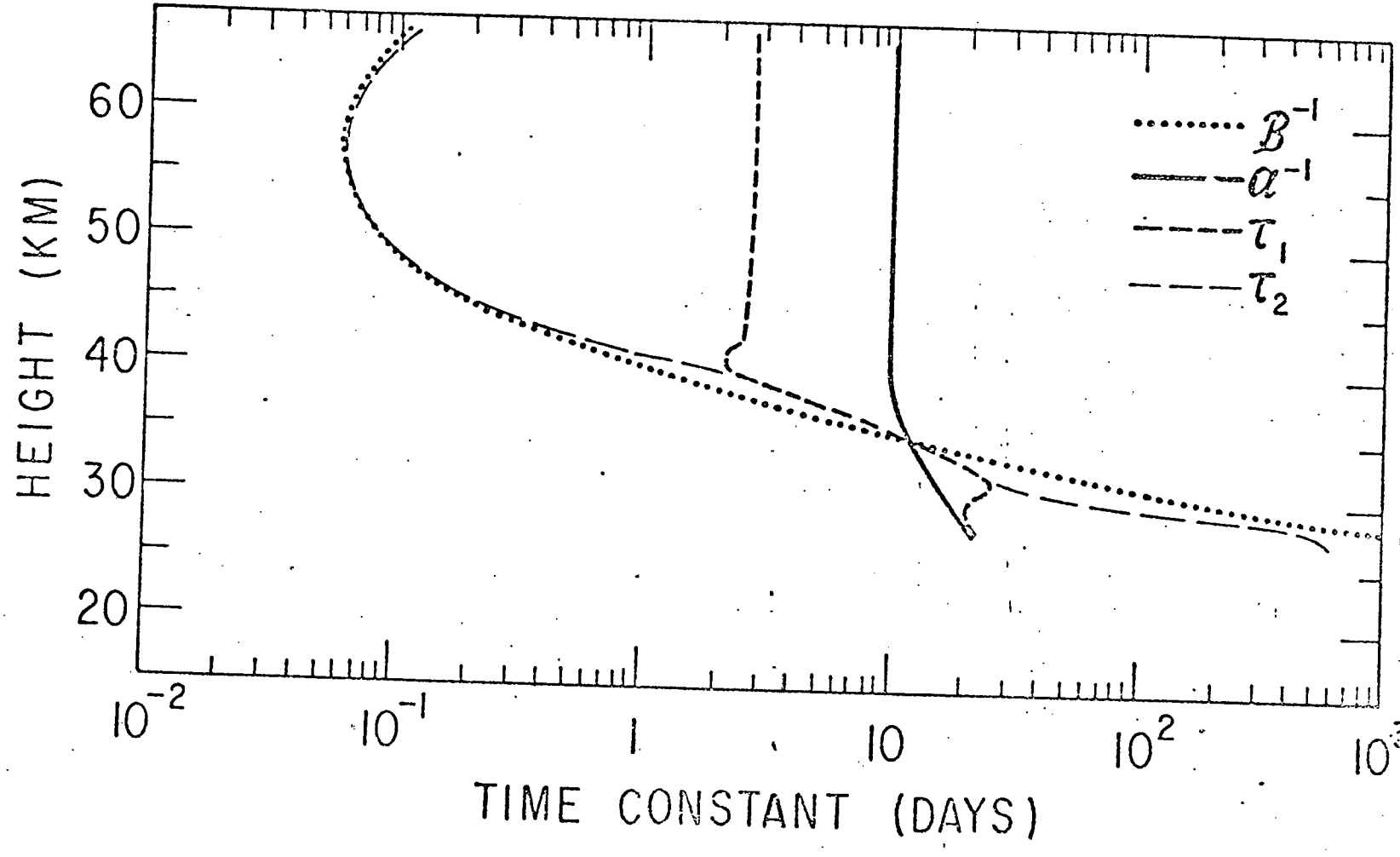
HEIGHT (KM)
60
50
40
30
20
10^{-2}
10^{-1}
1
10
10^{2}
10^{3}
TIME CONSTANT (DAYS)
$\mathcal{B}^{-1}$
α^{-1}
τ_1
τ_2

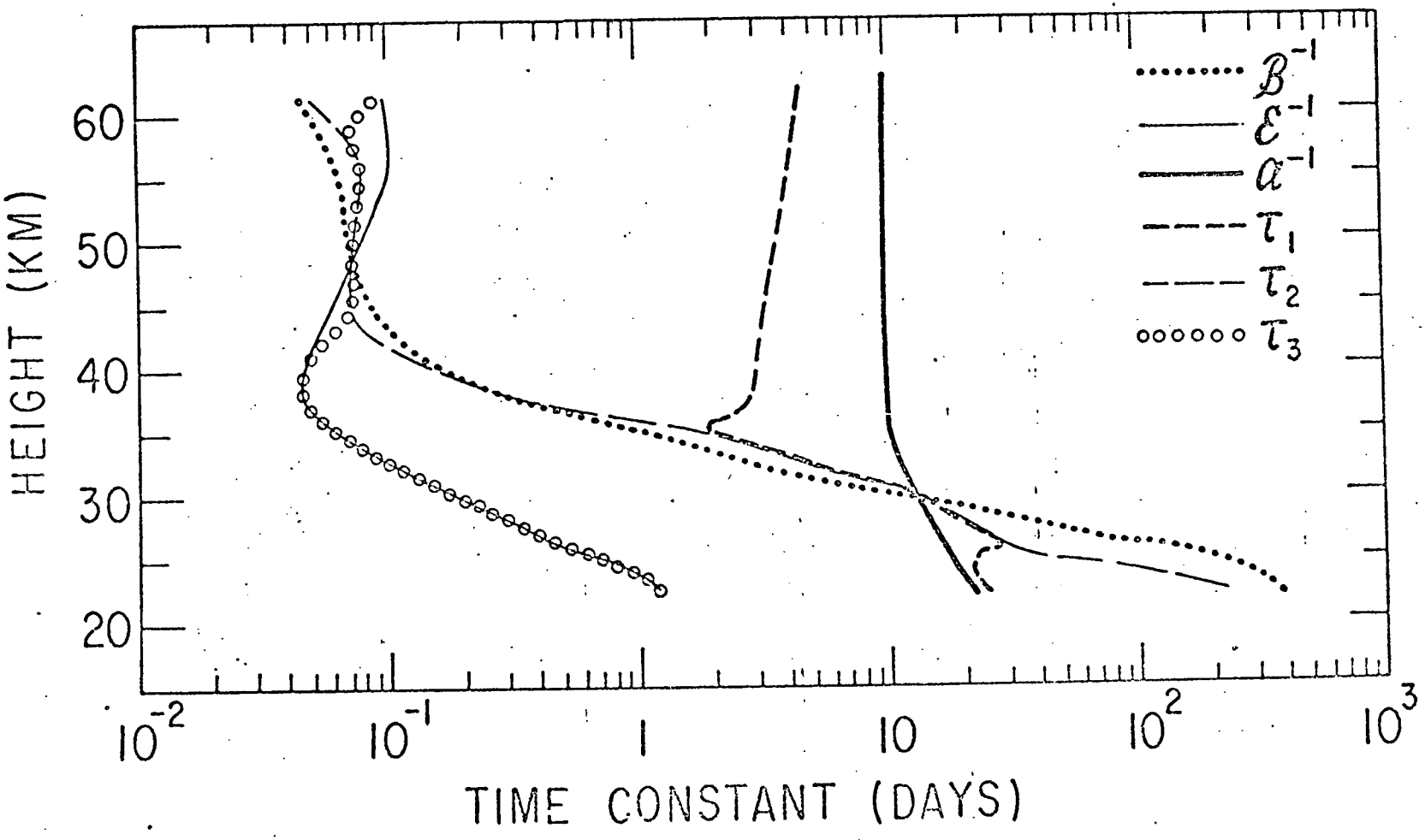
HEIGHT (KM)
60
50
40
30
20
10^{-2}
10^{-1}
1
10
10^{2}
10^{3}
TIME CONSTANT (DAYS)
$\mathcal{B}^{-1}$
$\mathcal{E}^{-1}$
α^{-1}
τ_1
τ_2
τ_3

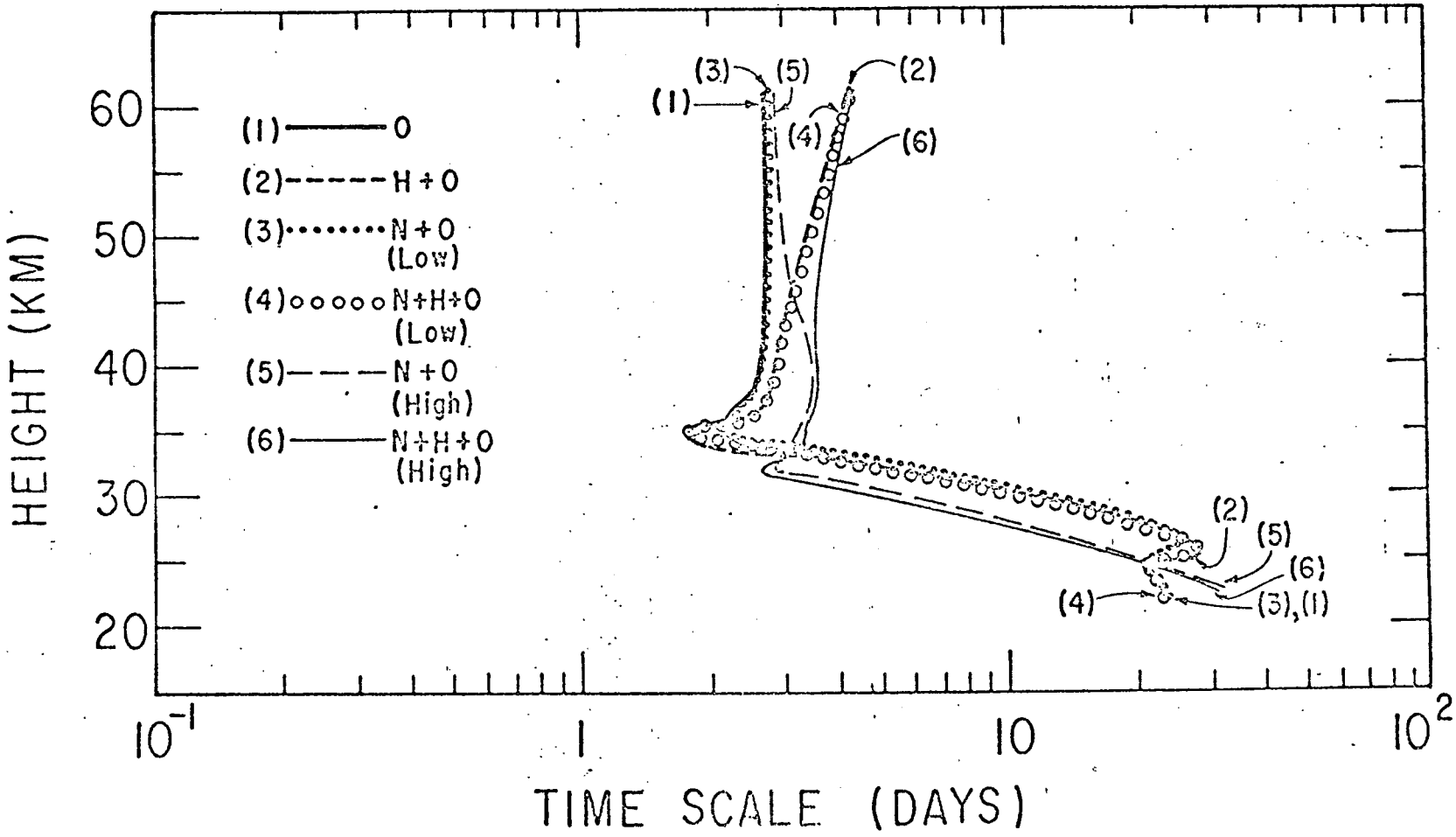
(1)——— O
(2)- - - - - H + O
(3)····· N + O (Low)
(4)ooooo N + H + O (Low)
(5)— — — N + O (High)
(6)——— N + H + O (High)
HEIGHT (KM)
60
50
40
30
20
10^{-1}
1
10
10^{2}
TIME SCALE (DAYS)
(1)
(2)
(3)
(4)
(5)
(6)
(3),(1)

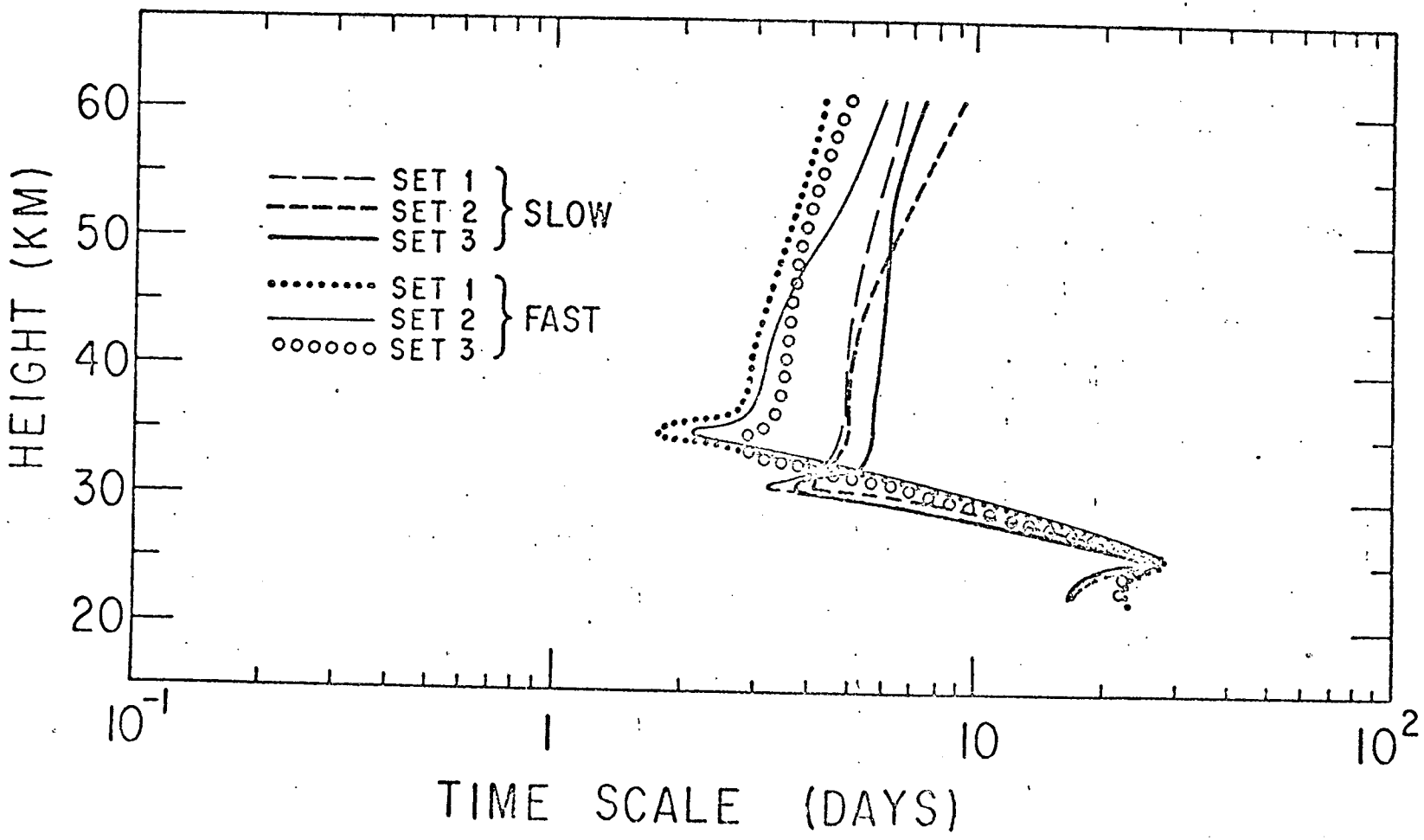
HEIGHT (KM)
60
50
40
30
20
SET 1
SET 2
SET 3
SLOW
SET 1
SET 2
SET 3
FAST
10^{-1}
1
10
10^2
TIME SCALE (DAYS)